Astronomy & Astrophysics manuscript no. propionitrile-D
November 7, 2008

Rotational spectrum of deuterated and ^{15}N ethyl cyanides: CH_3CHDCN and CH_2DCH_2CN and of $CH_3CH_2C^{15}N$. ⋆

L. Margulès[1], R. Motiyenko[1], K. Demyk[2], B. Tercero[3], J. Cernicharo[3], M. Sheng[4], M. Weidmann[4], J. Gripp[4], H. Mäder[4], and J. Demaison[1]

[1] Laboratoire de Physique des Lasers, Atomes et Molécules, UMR CNRS 8523, Université Lille 1, F-59655 Villeneuve d'Ascq Cedex, France
[2] Centre d'Etude Spatiale des Rayonnements, UMR CNRS 5187, Université de Toulouse (UPS), 9 avenue du Colonel Roche, BP 4346, F-31028 Toulouse, France
[3] Departamento de Astrofísica Molecular e Infrarroja, Instituto de Estructura de la Materia, CSIC, Calle Serrano 121, E-28006 Madrid, Spain
[4] Universität Kiel, Institut für Physikalische Chemie Olshausenstrasse 40, D-24098 Kiel , Germany

Received 2 September 2008; accepted 13 October 2008

ABSTRACT

Context. Ethyl cyanide is an abundant molecule in hot molecular clouds. Its rotational spectrum is very dense and several hundreds of rotational transitions within the ground state have been identified in molecular clouds in the 40 - 900 GHz frequency range. Lines from ^{13}C isotopically substituted ethyl cyanide were identified in Orion.
Aims. To enable the search and the possible detection of other isotopologues of ethyl cyanide in interstellar objects, we have studied the rotational spectrum of deuterated ethyl cyanide: CH_2DCH_2CN (in-plane and out-of-plane) and CH_3CHDCN and the spectrum of ^{15}N substituted ethyl cyanide $CH_3CH_2C^{15}N$. Using these experimental data, we have searched for these species in Orion.
Methods. The rotational spectrum of each species in the ground state was measured in the microwave and millimeter-submillimeter wavelength range using a waveguide Fourier transform spectrometer (8 - 17 GHz) and a source-modulated spectrometer employing backward-wave oscillators (BWOs) (150 - 260 and 580 - 660 GHz). More than 300 lines were identified for each species, for J values in the range 71-80 and K_a values in the range 28-31 depending on the isotopologues. The experimental spectra were analyzed using a Watson's Hamiltonian in the A-reduction.
Results. From the fitting procedure, accurate spectroscopic constants were derived for each of the species. These new sets of spectroscopic constants enable us to predict reliably the rotational spectrum (lines frequencies and intensities) in the 4-1000 GHz frequency range and for J and K_a up to 80 and 31, respectively. Combined with IRAM 30 m antenna observations of Orion, this experimental study allowed us to detect ^{15}N substituted ethyl cyanide $CH_3CH_2C^{15}N$ for the first time in Orion. The derived column density and rotational temperature are 10^{13} cm^{-2} and 150 K for the plateau and 3×10^{14} cm^{-2} and 300 K for the hot core. The deuterated species were searched for but were not detected. The upper limit to the column density of each deuterated isotopologues was 10^{14} cm^{-2}.

Key words. Line: identification – Methods: laboratory – Molecular data – ISM: molecules – Radio lines: ISM – Submillimeter

1. Introduction

Ethyl cyanide, CH_3CH_2CN, is an asymmetric top molecule with a large dipole moment (μ_a = 3.85 D and μ_b = 1.23 D) that exhibits a dense and intense rotational spectrum. It is present in the densest parts of hot molecular cores, where it is proposed to form on dust grains. Several hundreds of lines of CH_3CH_2CN in the ground state have been observed towards hot cores such as Orion, Sgr B2 and W51 (Miao & Snyder 1997; Liu et al. 2001) but also toward low mass star-forming regions (Cazaux et al. 2003; Remijan & Hollis 2006). It has a high abundance of the order of 10^{15} - 10^{17} cm^{-2} depending on the sources (Miao & Snyder 1997; Remijan et al. 2004; Remijan & Hollis 2006). Transitions from vibrationally excited ethyl cyanide have also been observed in Sgr B2 (Mehringer et al. 2004) and in W51 e2 (Demyk et al. 2008). Numerous lines from ^{13}C-substituted ethyl cyanide have been detected in Orion Irc2 (Demyk et al. 2007).

All of these observations show that the unidentified lines observed in spectral surveys of molecular clouds are partly due to transitions from known species in vibrationally excited states or from isotopologues of known species. The most promising carriers of these transitions are the so-called *interstellar weeds*, i.e. molecules, such as ethyl cyanide, which have a dense and intense rotational spectrum and/or low-frequency vibrational modes, such as methyl formate $HCOOCH_3$, dimethyl-ether CH_3OCH_3, or methanol CH_3OH. With the increase in sensitivity and frequency coverage that will be achieved with instruments such as HIFI onboard the Herschel Space Observatory and ALMA, the identification of these *U-lines* will become crucial to the search for new molecules but also to obtain important information about the physical and chemical conditions prevailing in the observed sources.

An enormous amount of experimental work must be undertaken to complete the actual knowledge of the rotational spectra of low-frequency vibrational mode and of the isotopologues of abundant interstellar molecules. When they exist, measurements

Send offprint requests to: K. Demyk, e-mail: karine.demyk@cesr.fr
⋆ Tables 7, 8, 9 and 10 are only available in electronic form at the CDS via anonymous ftp to cdsarc.u-strasbg.fr (130.79.125.5) or via http://cdsweb.u-strasbg.fr/cgi-bin/qcat?J/A+A/

are indeed often limited to low frequencies and therefore cannot be used to predict reliable line frequencies and intensities in the Herschel and ALMA frequency ranges.

In this context, following up our study on ^{13}C-substituted ethyl cyanide (Demyk et al. 2007), we present an experimental study of the rotational spectrum of deuterated ethyl cyanide, CH_2DCH_2CN in-plane, CH_2DCH_2CN out-of-plane, CH_3CHDCN, and ^{15}N substituted ethyl cyanide, $CH_3CH_2C^{15}N$. These species were studied 30 years ago by Mäder et al. (1973) and Heise et al. (1976). For each species, about 30 low-J ($J \leq 6$) rotational transitions were recorded and assigned in the 4 - 40 GHz frequency range. The rotational constants and quadrupole coupling constants derived from these studies were used to extend the measurements to higher frequency. The isotopologues synthesis and the experimental setup are described in Sect. 2. The analysis of the measured rotational transitions, the resulting spectroscopic parameters, and the prediction of rotational spectrum for each isotopologue in the 8 - 1000 GHz range are presented in Sect. 3. The detection of $CH_3CH_2C^{15}N$ in Orion and the search for the deuterated species is presented in Sect. 4.

2. Experimental setup

The deuterated ethyl cyanides, CH_2DCH_2CN and CH_3CHDCN, have been prepared from the corresponding ethyl iodides CH_2DCH_2I and CH_3CHDI (98 atom %, C/D/N isotopes, Pointe Claire, Canada) and normal potassium cyanide. $KC^{15}N$ (98 atom%, Aldrich, Taufkirchen, Germany) and normal ethyl iodide were used for the preparation of the ^{15}N- isotopologue. The potassium cyanide was dispersed in a solution of ethyl iodide in triethylene glycol and the mixture was stirred and heated slowly to 110 °C. Potassium cyanide and ethyl iodide were used in a molar ratio 1.25 : 1.00, and the concentration of the ethyl iodide solution was 4 mol/l. Nitrogen was bubbled through the mixture and the ethyl cyanide was isolated in an ice-cooled trap. The yield of this modified Kolbe reaction (Organikum 1977; Mäder et al. 1973) was 75%. The product was distilled and controlled spectroscopically. The only detectable impurity was a small amount of the corresponding isonitrile.

In Kiel, the measurements in the centimeter-wave range were performed by means of waveguide Fourier-transform microwave-spectroscopy (Sarka et al. 1997). A spectrometer in the range of about 8-17 GHz was used, employing an oversized X-band sample cell with a rectangular waveguide of quadratic cross-section and 12 m length (Krüger et al. 1993). The experiments were carried out at ambient temperature and at gas pressures of ca. 0.1 Pa. Experimental transition frequencies were obtained from an analysis of the frequency-domain signals; these were derived following Fourier transformation of the transient emission signal, using a peak finder routine that determined line-center frequencies to an accuracy typically superior to 20 kHz, depending on the strength of the line. In the case of observed line splittings due to methyl internal rotation (AE-splittings) and/or the ^{14}N-nuclear quadrupole coupling, the experimental peak frequencies were corrected to obtain hypothetical unsplit line frequencies (without nuclear quadrupole hyperfine structure).

The millimeter spectra were recorded in Lille in the spectral range 150 - 250 and 580 - 660 GHz. The sources were Russian Istok backward-wave oscillators (BWO). They were phase locked on an harmonic from a HP synthesizer. Up to 250 GHz, the signal from the synthesizer was directly mixed onto a Russian planar Schottky diode with part of the signal from the BWO. From 500 GHz to 650 GHz, an active sextupler from millitech (75 - 100 GHz) and a Schottky planar diode placed in a parabolic structure (from Virginia Diodes Inc.) optimized for this range were used. The detector was an InSb liquid He-cooled bolometer from QMC. To improve the sensitivity of the spectrometer, the sources were frequency-modulated at 5 kHz. The absorption cell was a stainless steel tube (6 cm diameter, 110 cm long), and the pressure that we used during measurements was 2.6 Pa (26 μbar). The accuracy of isolated lines was superior to 30 kHz.

3. Spectral analysis and line predictions

Ethyl cyanide and its isotopologues are prolate asymmetric top molecules. The main isotopologue, CH_3CH_2CN, has a large dipole moment (μ_a = 3.83 D, μ_b = 1.23 D; Heise et al. (1976)), which was used to calculate the lines intensities of the four studied isotopologues, since it was found that the rotation of the principal axes system upon isotopic substitution does not induce significant variation in the dipole moment. The experimental spectrum of each isotopologue is very dense and intense. It contains lines from the main isotopologue, which may be present as a trace in the samples. It also exhibits lines from the first low-frequency vibrationally excited states (the CH_3 torsion mode and the CCN bending mode). Consequently, some lines in the measured spectra are blended or distorded and are therefore not used in the analysis. ^{14}N-nuclear quadrupole coupling and the internal rotation of the CH_3 group introduce splitting of the lines. However, these effects were not taken into account in the analysis, since these splittings are not observed in the millimeter range, and in the microwave region the unsplit line frequencies are used when splitting is observed.

The spectral analysis is a step-by-step process with permanent interaction between measurements and theory. First of all, we used the spectroscopic parameters derived from previous experimental studies at low frequency (4 - 40 GHz) to provide a first prediction of the line positions at low frequency and for low J and K_a value for each species. We used the experimental work from Heise et al. (1976) and Mäder et al. (1976) for $CH_3CH_2C^{15}N$ and CH_2DCH_2CN, respectively. The quartic distortional constants missing (δ_J and δ_K) were fixed to the values of the normal species. In the absence of any experimental data, the rotational constants of CH_3CHDCN, were calculated using ab initio calculation at the level B3LYP/6-31G* with Gaussian 03 (Frisch et al. 2004). Based on these predictions, new lines were identified in new measurements performed in the 8 - 17 GHz range. All of the measured lines were then fitted to derive a new and more accurate set of spectroscopic constants. These constants were then used to derive a new prediction at higher frequency and for a higher value of J and K_a. New lines were measured and added to the fit step by step until the fit of the measured lines and the precision of the derived spectroscopic parameters were sufficiently good for a reliable prediction to be made for the desired frequency range and value of quantum numbers. For the fitting procedure of the measured lines and for the predictions, we have used a Watson's Hamiltonian using A-reduction in I^r representation (Watson 1977). The S reduction was also attempted but without significant improvement (as for the ^{13}C species, Demyk et al. (2007)). The molecular parameters were determined by fitting the experimental frequencies using the iteratively re-weighted least squares fitting method (Hamilton 1992; Bakri et al. 2002).

The objective of this method was to derive suitable weights using the residuals of a previous iteration. It had the advantage of being more robust than the standard least squares fitting methods and automatically rejecting most of the misassigned lines.

The number of measured lines, the maximum value of J and K_a, and the standard deviation of the fits are presented in Table 1 for the four studied species: $CH_3CH_2C^{15}N$, CH_2DCH_2CN in-plane, CH_2DCH_2CN out-of-plane, and CH_3CHDCN. For the $CH_3CH_2C^{15}N$ and CH_3CHDCN species, it is possible to reduce the standard deviation of the fit slightly by using higher order centrifugal distortion constants; but they are only marginally determined and they worsen the precision of the predictions. They were therefore no longer considered. The spectroscopic parameters derived from the fitting procedure are presented in Table 2. The list of measured lines are accessible in the online section as Tables 3, 4, 5, and 6 for $CH_3CH_2C^{15}N$, CH_3CHDCN, CH_2DCH_2CN in-plane, and CH_2DCH_2CN out-of-plane, respectively. For each measured line, the tables indicate its assignment (quantum numbers), the measured frequency, the difference between the observed and calculated frequency, the line strength, the dipole component, and the energy of the lower level.

The frequency range of the measurements (8 - 660 GHz) and the value of the quantum numbers of the identified lines ($J \leq 80$ and $K_a \leq 31$) are suitable for astronomical studies. Ethyl cyanide is present in hot cores and has a rather high temperature, in the 100 - 300 K range, as its isotopologues should also have. For such temperatures (100 and 300 K), the most intense rotational transitions of ethyl cyanide occur around 238 and 407 GHz, respectively, corresponding to J values of 25 and 45, respectively. The set of spectroscopic parameters derived for each species thus allows us to predict reliably the line frequencies and the band intensity of the transitions in the spectral range suitable for interstellar detection. For each species we have calculated a prediction of the rotational spectrum in the 8 - 1000 GHz range for $J \leq 100$ and $K_a \leq 35$. A short sample of the predictions is shown in the online section for each isotopologues (Tables 7, 8, 9 and 10), the entire tables are available in electronic form at the CDS. The tables indicate the quantum numbers of the transition, the calculated frequency and uncertainty, the line strength, the dipole component and the energy of the lower level. The calculated error (third column in the tables) is estimated from the accuracy of the spectroscopic parameters derived by the fitting procedure. However, to get a more realistic estimation of the error, it must be multiplied by a factor 3 for the strongest lines to 10, for the weakest lines. The precision on the line frequency is good enough for line identification in interstellar spectra. For the lines that are the most suitable for detection, i.e., the strongest lines having J value up to ∼ 50-60 and a low K_a value, the error on the predicted frequencies is a few hundred kHz. The error is larger for the weakest lines and increases as J and K_a become larger, i.e., as the frequency increases.

4. $CH_3CH_2C^{15}N$ detection in Orion

4.1. Astronomical observation

The observations were carried out using the IRAM 30 m radio telescope during 2004 September (3 mm and 1.3 mm), 2005 March (2 mm), 2005 April (3 mm and 1.3 mm). We acquired data for the entire spectral range detectable by the 30-m recievers. The four SiS receivers operating at 3, 2 and 1.3 mm were used simultaneously. Each receiver was tuned to a single sideband with image rejections within 20-27 dB (3 mm receivers), 12-16 dB (2 mm receivers), and 13 dB (1.3 mm receivers).

System temperatures were 100-350 K for the 3 mm receivers, 200-500 K for the 2 mm receivers, and 200-800 K for the 1.3 mm receivers, depending on the particular frequency, weather conditions, and source elevation. The intensity scale was calibrated using two absorbers at different temperatures and using the Atmospheric Transmission Model (Cernicharo 1985; Pardo et al. 2001).

Pointing and focus were regularly monitored by observing the nearby quasars 0420-014 and 0528+134. The observations were completed in the balanced wobbler-switching mode with a wobbling frequency of 0.5 Hz and a beam throw in azimuth of ±240”. The backends used were two filter banks with 512×1 MHz channels and a correlator providing two 512 MHz bandwidths and 1.25 MHz resolution. We performed a spectral-line survey, for which the central frequencies were chosen in a systematic way: from 80 GHz to 115.5 GHz for the 3 mm domain; from 130.25 GHz to 176.75 GHz for 2 mm; from 197 to 141 GHz for 1.3 mm (low frequency) and from 141.25 to 281.75 GHz for the 1.3 mm domain (high frequency), in steps of 500 MHz. We pointed toward the (survey) position $\alpha = 5^h\ 35^m\ 14.5^s$, $\delta = -5°\ 22'\ 30.0''$ (J2000.0), corresponding to IRc2. The detailed procedure used for the analysis of the line survey is described in Tercero et al. (in preparation).

4.2. Astronomical modeling

In agreement with previous observations of Orion, four clearly defined kinematic regions with quite different physical and chemical conditions (Blake et al. 1987, 1996) are implied by the observed LSR velocities and line widths: (i) the narrow ($\lesssim$5 km s^{-1} line width) feature at $v_{LSR} \simeq 9$ km s^{-1}, forming a N-S *extended ridge* or ambient cloud; (ii) a compact and quiescent region, *compact ridge*, ($v_{LSR} \simeq 8$ km s^{-1}, $\Delta v \simeq 3$ km s^{-1}), identified for the first time by Johansson et al. (1984); (iii) the more turbulent and compact *plateau* ($v_{LSR} \simeq$ 6-10 km s^{-1}, $\Delta v \gtrsim$25 km s^{-1}); (iv) the *hot core* component ($v_{LSR} \simeq$ 3-5 km s^{-1}, $\Delta v \lesssim$10-15 kms^{-1}), first observed in ammonia emission (Morris et al. 1980).

In modeling the emission from the ^{15}N isotopologue of ethyl cyanide, we found that, as for the ^{13}C isotopologues (Demyk et al. 2007), a sum of two components is sufficient to reproduce all line intensities and profiles reasonably well: the hot core component and the plateau. We assumed LTE for both components. For the hot core, a column density of 3×10^{14} cm^{-2}, a line width of 5 km s^{-1}, and a rotational temperature of 300 K were the most suitable parameters for reproducing the bulk of the $CH_3CH_2C^{15}N$ emission. A broad velocity component is was also required to reproduce the observations accurately, corresponding to the plateau for which we obtain a column density of 1×10^{13} cm^{-2}, a line width of 20 km s^{-1}, and a rotational temperature of 150 K. For the hot core component, we assumed a source diameter of 7” with uniform brightness temperature and optical depth over its extent at 3” from the pointed position (the observation were pointed towards IRc2, while the CN bearing species appears to originate in a small region 3” North). For the plateau component, we assumed a size for the source of 30”.

The lines of $CH_3CH_2C^{15}N$ are weak and many of them are heavily blended with lines from other species. However, no

Table 1. Spectroscopic measurements of the ground vibrational state of CH_3CHDCN, CH_2DCH_2CN and $CH_3CH_2C^{15}N$

	Number of measured lines 8-39 GHz	150-660 GHz	J max	K_a max	standard deviation[a] (kHz)
CH_2DCH_2CN in-plane	45	415	80	28	27
CH_2DCH_2CN out-of plane	58	496	74	29	28
CH_3CHDCN	55	222	71	29	57[b]
$CH_3CH_2C^{15}N$	67	270	78	31	64[b]

[a] calculated from the median of absolute deviations

[b] For the millimeter wave transitions, the standard deviation of the microwave transitions is 16 kHz.

Table 2. Spectroscopic constants of the ground vibrational state of CH_3CHDCN, CH_2DCH_2CN and $CH_3CH_2C^{15}N$

	CH_2DCH_2CN in-plane	CH_2DCH_2CN out-of-plane	CH_3CHDCN	$CH_3CH_2C^{15}N$
A /MHz	27651.28641(85)	25022.90806(62)	24449.0602(15)	27541.8853(13)
B /MHz	4425.144021(82)	4583.488572(88)	4661.39671(21)	4574.82824(19)
C /MHz	4000.798104(76)	4110.239468(83)	4155.45941(20)	4119.44781(19)
Δ_J /kHz	2.565394(33)	3.122672(31)	2.839982(82)	2.893555(79)
Δ_{JK} /kHz	-45.12388(92)	-39.91080(59)	-34.0809(14)	-46.1359(13)
Δ_K /kHz	551.5425(70)	405.8505(38)	365.720(24)	547.265(14)
δ_j /Hz	550.855(23)	703.046(20)	656.296(27)	635.249(38)
δ_k /kHz	10.8468(55)	11.0888(26)	11.6287(44)	12.5398(81)
Φ_J /mHz	7.5447(37)	9.9689(35)	8.4837(98)	8.9909(84)
Φ_{JK} /mHz	-54.29(79)	-34.13(73)	-	-20.9(11)
Φ_{KJ} /Hz	-1.3293(42)	-1.3663(31)	-1.1188(27)	-1.9066(62)
Φ_K /Hz	28.440(21)	18.8395(90)	15.57(10)	30.827(44)
ϕ_j /mHz	2.8196(28)	3.8411(23)	3.3694(40)	3.4096(49)
ϕ_{jk} /mHz	78.25(65)	101.06(39)	85.03(74)	103.26(85)
ϕ_k /Hz	5.618(63)	4.153(46)	4.067(12)	6.561(84)
L_{JK} /MHz	-	-	-	-6.45(27)
L_{KKJ} /MHz	38.7(27)	48.04(99)	-	101.5(24)
l_k /MHz	279.(14)	236.7(61)	317.(14)	-

Standard deviation of the fits are given Table 1, see text for more details. Uncertainties given in parenthesis are in units of the last digit given and 1 times the standard deviation.

missing lines were found in the coverage of our line survey of Orion and the lines of $CH_3CH_2C^{15}N$ free of blending appear at the correct frequencies and with the correct intensities. Although our modeling lacks a robust analysis, the difference between model and observed intensities is always below 20%. Our modeling of the different components is straightforward, although we emphasize that we modeled the main isotope, for which strong lines are observed, with the same model and the lines are well reproduced. Hence, we are confident about the results for the isotope ^{15}N, in particular that the frequency of all detected lines differ from laboratory measurements by less than 0.5 MHz. Hence, our assignment of the lines shown in Fig. 1 and in Table 11 to the ^{15}N isotopologue is fairly secure. The procedure that we used to identify the carriers of the weak lines in Orion, many of which remain unassigned at present, is the most suitable for this source since it permits to confirm whether there are no missing lines of the molecules for which we are looking.

Fig. 1 shows selected observed lines of the ^{15}N isotopologue with model results. Table 11 indicates the model predictions, observed peak intensities and frequencies, and predicted frequencies from the rotational constants obtained in this paper, for all lines of $CH_3CH_2C^{15}N$ that were not strongly blended with other lines. The differences between the intensity of the model and the peak intensity of the observed lines were mostly due to the contribution from many other molecular species (the strong overlap with other lines ensures that it is difficult to provide a good baseline for the weak lines of $CH_3CH_2C^{15}N$).

Using the column density derived for the ^{13}C isotopologues (1.6×10^{15} and 6×10^{13} cm^{-2} for the hot core and the plateau, respectively; see Demyk et al. 2007), we derive an isotopic ratio $^{13}C/^{15}N$ of between 5-6, in agreement with the solar isotopic abundance ($^{13}C/^{15}N$ (solar) $\simeq$ 6) and strengthening our identification of ^{15}N-ethyl cyanide in Orion. The detailed modeling of ethyl cyanide including the main isotopologue, the vibrationally excited states and the detected isotopologues, will be published elsewhere (Tercero et al. in preparation).

Deuterated ethyl cyanide has not been detected in this line survey above the line confusion limit. Assuming the same physical conditions as those derived for $CH_3CH_2C^{15}N$, we have derived an upper limit to the column densities of CH_2DCH_2CN (in-plane and out-of-plane) of 1×10^{14} cm^{-2} in both species.

Acknowledgements. This work was supported by the Programme National "Physico Chimie du Milieu Interstellaire" and by the European Research Training Network "Molecular Universe" (MRTN-CT-2004-512302). R.M. has been supported by INTAS young research fellowship. The Kiel authors thank the Land Schleswig-Holstein for financial support.

References

Bakri, B., Demaison, J., Kleiner, I., et al. 2002, Journal of Molecular Spectroscopy, 215, 312
Blake, G. A., Mundy, L. G., Carlstrom, J. E., et al. 1996, ApJ, 472, L49+
Blake, G. A., Sutton, E. C., Masson, C. R., & Phillips, T. G. 1987, ApJ, 315, 621
Cazaux, S., Tielens, A. G. G. M., Ceccarelli, C., et al. 2003, ApJ, 593, L51
Cernicharo, J. 1985, Internal IRAM report (Granada: IRAM)
Demyk, K., Mäder, H., Tercero, B., et al. 2007, A&A, 466, 255
Demyk, K., Wlodarczak, G., & Carvajal, M. 2008, submitted to A&A
Frisch, M., Trucks, G. W., Schlegel, H. B., et al. 2004, Gaussian 03, Revision D.01 (Gaussian, Inc., Wallingford CT)
Hamilton, L. 1992, Regression with graphics (Duxbury Press, Belmont, CA)

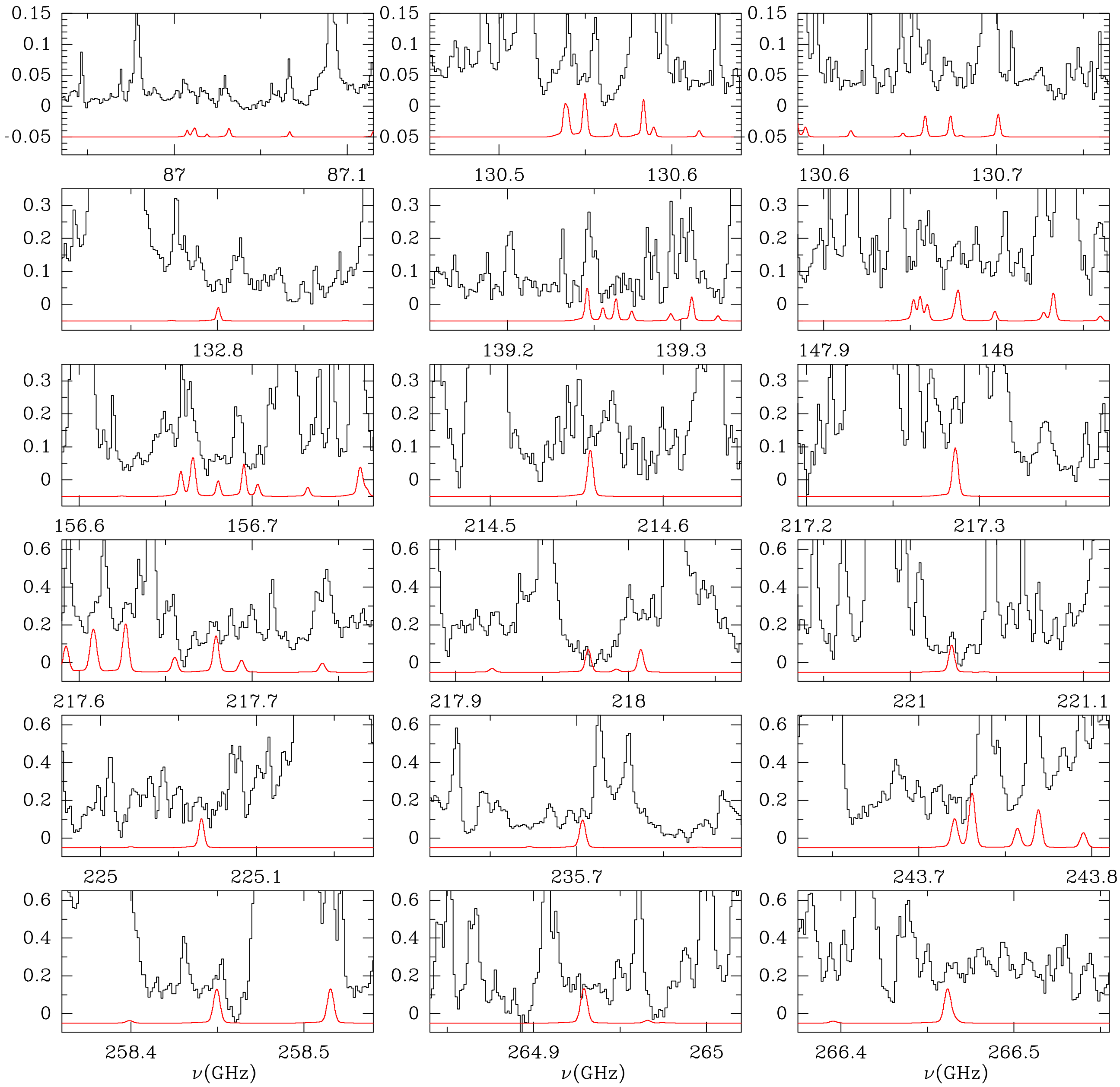

Fig. 1. ^{15}N-ethyl cyanide isotopologues detection in Orion. The spectra are in units of main beam temperature (T_{mb}). The histogram spectra offset with respect to each other are the observations (black curve) and the model (smooth red line).

Heise, H. M., Mäder, H., & Dreizler, H. 1976, Zeitschrift Naturforschung Teil A, 31a, 1398
Johansson, L. E. B., Andersson, C., Ellder, J., et al. 1984, A&A, 130, 227
Krüger, M., Harder, H., Gerke, C., & H., D. 1993, Zeitschrift Naturforschung Teil A, 48, 737
Liu, S.-Y., Mehringer, D. M., & Snyder, L. E. 2001, ApJ, 552, 654
Mäder, H., Heise, H. M., & Dreizler, H. 1973, Zeitschrift Naturforschung Teil A, 29a, 164
Mäder, H., Heise, H. M., & Dreizler, H. 1976, Zeitschrift Naturforschung Teil A, 29a, 1228
Mehringer, D. M., Pearson, J. C., Keene, J., & Phillips, T. G. 2004, ApJ, 608, 306
Miao, Y. & Snyder, L. E. 1997, ApJ, 480, L67+
Morris, M., Palmer, P., & Zuckerman, B. 1980, ApJ, 237, 1
Organikum, A. 1977 (Auflage S.269 VEB Deutscher Verlag der Wissenschaften Berlin)
Pardo, J. R., Cernicharo, J., & Serabyn, E. 2001, IEEE Transactions on Antennas and Propagation, 49, 1683
Remijan, A., Shiao, Y.-S., Friedel, D. N., Meier, D. S., & Snyder, L. E. 2004, ApJ, 617, 384
Remijan, A. J. & Hollis, J. M. 2006, ApJ, 640, 842
Sarka, K., Papoušek, D., Demaison, J., & Mäder, H. 1997, Advanced Series in Physical Chemistry, d. papoušek edn., Vol. 9 (Singapore: World Scientic Publishing)
Watson, J. K. G. 1977, Vibrational Spectra and Molecular Structure, d. papoušek edn., Vol. 6 (Elsevier, Amsterdam), 1

Online Material

Table 3. Measured transitions of the ground vibrational state of $CH_3CH_2C^{15}N$

Transition						Obs. Freq.	obs.- calc.	S	Dipole	E_l
J'	K'$_a$	K'$_c$	J"	K"$_a$	K"$_c$	(MHz)	(MHz)			(cm^{-1})
13	2	11	13	2	12	8439.616	0.003	5.5270	a	29.44
27	6	22	28	5	23	8579.609	-0.004	4.3669	b	137.32
1	0	1	0	0	0	8694.274	0.010	1.0000	a	0.00
27	6	21	28	5	24	8864.577	0.008	4.3657	b	137.31
31	4	27	31	4	28	9029.287	-0.011	0.8976	a	156.65
30	5	26	29	6	23	9223.293	-0.017	4.7882	b	154.18
61	7	54	61	7	55	9230.917	-0.004	1.3312	a	587.92
7	2	5	8	1	8	9270.407	0.020	1.0280	b	10.93
22	3	19	22	3	20	9468.661	-0.003	0.7197	a	80.47
6	1	5	6	1	6	9554.530	0.005	0.3102	a	6.70
41	5	36	41	5	37	9774.927	-0.010	1.0376	a	269.87
30	5	25	29	6	24	9780.015	-0.010	4.7908	b	154.17
51	6	45	51	6	46	9786.557	0.007	1.1824	a	413.66
15	2	14	14	3	11	9904.529	-0.014	2.2952	b	37.48
46	8	39	45	9	36	10289.690	0.000	7.3345	b	363.08
46	8	38	45	9	37	10303.589	-0.022	7.3346	b	363.08
14	2	12	14	2	13	10999.282	0.002	0.5055	a	33.48
62	7	55	62	7	56	11195.294	-0.016	1.2899	a	605.99
25	4	22	24	5	19	11277.619	0.002	4.0009	b	106.47
32	4	28	32	4	29	11288.624	-0.010	0.8540	a	165.97
32	7	26	33	6	27	11296.821	0.000	5.1435	b	190.82
32	7	25	33	6	28	11373.145	0.036	5.1432	b	190.82
16	4	13	17	3	14	11475.918	0.001	2.6021	b	51.48
12	1	12	11	2	9	11634.396	-0.012	1.2301	b	22.36
52	6	46	52	6	47	11946.306	0.015	1.1406	a	428.82
23	3	20	23	3	21	11978.970	-0.011	0.6755	a	87.15
42	5	37	42	5	38	12042.892	-0.022	0.9951	a	282.11
20	3	18	19	4	15	12079.320	0.008	3.1893	b	67.57
5	2	4	6	1	5	12719.608	0.008	0.9101	b	7.02
7	1	6	7	1	7	12732.353	0.003	0.2689	a	8.68
4	0	4	3	1	3	12851.255	0.004	1.6107	b	2.47
41	7	35	40	8	32	13094.510	-0.015	6.5569	b	287.57
11	3	8	12	2	11	13420.087	0.028	1.7745	b	25.68
63	7	56	63	7	57	13500.281	0.023	1.2487	a	624.34
14	2	12	13	3	11	13834.054	0.009	2.3230	b	33.39
33	4	29	33	4	30	13961.689	-0.009	0.8118	a	175.57
37	8	30	38	7	31	13970.932	-0.011	5.9196	b	253.11
37	8	29	38	7	32	13990.537	0.003	5.9195	b	253.11
15	2	13	15	2	14	14012.666	-0.001	0.4639	a	37.81
53	6	47	53	6	48	14483.258	-0.006	1.0990	a	444.27
43	5	38	43	5	39	14713.143	-0.014	0.9534	a	294.64
21	5	17	22	4	18	14851.715	-0.007	3.3752	b	85.92
24	3	21	24	3	22	14935.533	-0.007	0.6340	a	94.12
13	1	13	12	2	10	15425.057	-0.014	1.2023	b	25.89
21	5	16	22	4	19	15563.277	0.004	3.3716	b	85.89
6	2	4	7	1	7	15696.387	0.017	0.8951	b	8.68
36	6	31	35	7	28	15803.117	0.011	5.7777	b	220.84
36	6	30	35	7	29	16013.770	0.026	5.7786	b	220.84
64	7	57	64	7	58	16186.292	0.012	1.2076	a	642.99
8	1	7	8	1	8	16356.925	-0.004	0.2377	a	10.93
52	9	44	51	10	41	16396.371	-0.013	8.3221	b	462.17
42	9	34	43	8	35	16671.014	-0.002	6.6953	b	324.19
10	3	8	11	2	9	16882.196	0.004	1.6202	b	22.36
2	1	2	1	1	1	16933.357	0.023	1.5000	a	1.06
34	4	30	34	4	31	17086.864	0.039	0.7710	a	185.47
16	2	15	15	3	12	17185.449	-0.005	2.4300	b	41.85
2	0	2	1	0	1	17381.760	0.002	0.4273	a	42.42
16	2	14	16	2	15	17495.223	0.009	1.9999	a	0.29

continued on next page

Table 3 Measured transitions of $CH_3CH_2C^{15}N$– continued from previous page

Transition						Obs. Freq.	obs.- calc.	S	Dipole	E_l
J'	K'$_a$	K'$_c$	J"	K"$_a$	K"$_c$	(MHz)	(MHz)			(cm^{-1})
2	1	1	1	1	0	17843.970	0.016	1.5000	a	1.07
1	1	0	1	0	1	23422.150	0.195	1.5000	b	0.29
2	1	1	2	0	2	23884.160	0.009	2.4753	b	0.87
3	1	2	3	0	3	24589.950	0.017	3.4137	b	1.74
3	1	3	2	1	2	25395.730	0.020	2.666	a	1.62
3	0	3	2	0	2	26055.770	0.050	2.9994	a	0.87
3	2	2	2	2	1	26083.700	0.077	1.6667	a	3.96
3	2	1	2	2	0	26110.300	-0.118	1.6667	a	3.96
3	1	2	2	1	1	26761.440	-0.062	2.6666	a	1.67
1	1	1	0	0	0	31660.920	0.026	2.6666	b	0.00
2	1	2	1	0	1	39899.960	-0.004	1.5000	b	0.29
20	1	20	19	1	19	167736.896	0.066	1.5000	a	54.16
20	0	20	19	0	19	168308.099	0.086	19.9316	a	54.05
20	2	19	19	2	18	172402.970	0.120	19.9403	a	57.98
20	8	13	19	8	12	174074.577	0.088	19.7808	a	104.59
20	9	12	19	9	11	174075.603	0.101	16.8004	a	117.71
20	10	11	19	10	10	174088.863	0.086	15.9504	a	132.35
20	7	14	19	7	13	174091.333	0.102	15.0004	a	93.02
20	11	9	19	11	8	174111.289	0.044	17.5504	a	148.52
20	6	14	19	6	13	174136.505	0.003	13.9503	a	82.98
20	6	15	19	6	14	174136.505	0.094	18.2003	a	82.98
20	12	9	19	12	8	174141.113	0.035	18.2003	a	166.22
20	13	7	19	13	6	174177.165	0.041	12.8003	a	185.43
20	14	6	19	14	5	174218.677	0.051	11.5503	a	206.16
20	5	16	19	5	15	174231.742	0.016	10.2002	a	74.50
20	5	15	19	5	14	174235.852	0.023	18.7502	a	74.50
20	15	6	19	15	5	174265.094	0.029	18.7502	a	228.39
20	3	18	19	3	17	174273.451	0.100	8.7502	a	62.16
20	16	4	19	16	3	174316.107	0.033	19.5460	a	252.13
20	17	3	19	17	2	174371.426	0.042	7.2002	a	277.36
20	4	17	19	4	16	174391.672	0.068	5.5501	a	67.56
20	19	1	19	19	0	174494.185	0.048	19.1996	a	332.27
20	4	16	19	4	15	174501.063	0.113	1.9500	a	67.57
20	3	17	19	3	16	175670.653	0.064	19.1996	a	62.30
21	0	21	20	0	20	176494.285	0.054	19.5487	a	59.67
20	2	18	19	2	17	177778.527	0.026	20.9391	a	59.00
22	0	22	21	0	21	184683.451	0.089	19.8087	a	65.55
21	3	18	20	3	17	184690.770	0.072	21.9381	a	68.16
23	1	23	22	1	22	192539.029	0.046	20.5706	a	71.78
23	0	23	22	0	22	192876.014	0.075	22.9334	a	71.71
18	2	17	17	1	16	193737.725	-0.040	22.9373	b	46.05
22	3	19	21	3	18	193741.168	-0.069	7.2189	a	74.32
37	3	35	37	2	36	193807.027	-0.155	21.5910	b	204.24
23	1	23	22	0	22	194359.838	0.062	14.1553	b	71.71
9	3	6	8	2	7	194740.388	0.127	18.9865	b	13.53
23	2	22	22	2	21	197751.274	0.129	3.4828	a	76.07
23	9	15	22	9	14	200193.855	0.113	22.7981	a	136.00
23	10	14	22	10	13	200201.229	0.082	19.4787	a	150.64
23	8	16	22	8	15	200203.741	0.098	18.6526	a	122.88
23	11	13	22	11	12	200221.198	0.007	20.2178	a	166.82
23	7	17	22	7	16	200239.243	0.015	17.7396	a	111.31
23	12	12	22	12	11	200251.135	0.036	20.8700	a	184.52
23	13	10	22	13	9	200289.205	0.076	16.7395	a	203.73
23	3	21	22	3	20	200307.620	0.082	15.6525	a	80.47
23	14	9	22	14	8	200334.120	-0.015	22.6012	a	224.47
23	15	9	22	15	8	200385.331	-0.008	14.4786	a	246.70
23	1	22	22	1	21	200425.298	0.050	13.2177	a	75.29
23	16	7	22	16	6	200442.189	-0.002	22.8741	a	270.44
23	5	19	22	5	18	200466.463	0.129	11.8698	a	92.81
23	5	18	22	5	17	200480.816	0.035	21.9131	a	92.81

continued on next page

Table 3 Measured transitions of $CH_3CH_2C^{15}N$– continued from previous page

Transition						Obs. Freq.	obs.- calc.	S	Dipole	E_l
J'	K'$_a$	K'$_c$	J"	K"$_a$	K"$_c$	(MHz)	(MHz)			(cm^{-1})
23	17	6	22	17	5	200504.312	0.022	21.9131	a	295.68
23	18	5	22	18	4	200571.389	0.053	10.4350	a	322.40
23	19	4	22	19	3	200643.145	0.046	8.9133	a	350.60
23	4	20	22	4	19	200669.063	0.120	7.3045	a	85.89
29	5	24	29	4	25	200693.272	-0.036	22.3034	b	139.07
23	20	3	22	20	2	200719.345	-0.051	16.0583	a	380.28
24	1	24	23	1	23	200793.296	0.102	5.6088	a	78.20
23	21	2	22	21	1	200800.105	0.026	23.9337	a	411.42
23	22	1	22	22	0	200885.025	-0.001	3.8262	a	444.03
23	4	19	22	4	18	200952.117	0.023	1.9566	a	85.92
28	5	23	28	4	24	202003.528	-0.075	22.3036	b	130.58
24	1	24	23	0	23	202277.181	0.150	15.3800	b	78.15
23	3	20	22	3	19	202817.910	0.055	20.0098	a	80.79
27	5	22	27	4	23	203124.417	-0.017	22.6101	b	122.39
26	5	21	26	4	22	204076.918	-0.055	14.7154	b	114.50
23	2	21	22	2	20	204419.505	0.010	14.0626	a	77.68
25	5	20	25	4	21	204881.818	0.014	22.8303	b	106.91
24	5	19	24	4	20	205558.318	0.022	13.4202	b	99.62
31	5	27	31	4	28	205711.989	-0.056	12.7872	b	156.65
32	5	28	32	4	29	205713.735	0.039	17.2162	b	165.97
30	5	26	30	4	27	205774.851	-0.004	17.8631	b	147.62
33	5	29	33	4	30	205793.562	-0.068	16.5700	b	175.57
29	5	25	29	4	26	205889.044	-0.077	18.5090	b	138.88
34	5	30	34	4	31	205966.280	-0.025	15.9257	b	185.47
23	5	19	23	4	20	207061.424	0.037	19.1522	b	92.59
22	5	18	22	4	19	207264.077	0.082	12.1465	b	85.89
20	5	15	20	4	16	207308.973	-0.035	11.5344	b	73.39
21	5	17	21	4	18	207454.740	-0.039	10.3294	b	79.49
36	4	33	36	2	34	207629.152	-0.065	10.9273	a	199.21
20	5	16	20	4	17	207630.890	-0.121	0.1443	b	73.38
38	5	34	38	4	35	207884.134	-0.016	10.3249	b	227.95
18	5	14	18	4	15	207933.343	-0.077	21.6546	b	62.04
17	5	12	17	4	13	207966.998	0.145	9.1323	b	56.81
17	5	13	17	4	14	208058.204	-0.094	8.5419	b	56.81
16	5	11	16	4	12	208108.794	0.004	8.5409	b	51.87
27	1	27	26	1	26	225525.534	0.024	7.9523	a	99.12
27	0	27	26	0	26	225679.061	0.088	26.9341	a	99.09
48	5	44	48	4	45	225893.897	-0.039	26.9355	b	354.12
45	6	39	45	5	40	228751.245	0.064	26.5948	b	321.29
49	5	45	49	4	46	228977.623	0.001	26.6357	b	368.28
43	6	37	43	5	38	234586.186	0.030	26.9371	b	295.13
27	3	25	26	3	24	234807.785	-0.021	24.9776	a	108.93
27	10	18	26	10	17	235016.788	0.026	26.6513	a	179.10
27	9	19	26	9	18	235022.338	0.008	23.2969	a	164.45
27	11	17	26	11	16	235029.774	-0.019	24.0006	a	195.28
27	8	20	26	8	19	235054.039	-0.028	22.5191	a	151.34
27	12	15	26	12	14	235056.914	-0.022	24.6302	a	212.98
27	13	14	26	13	13	235095.448	0.066	21.6672	a	232.20
27	7	21	26	7	20	235125.658	0.037	20.7412	a	139.77
27	14	14	26	14	13	235143.241	-0.052	25.1857	a	252.94
27	15	12	26	15	11	235199.461	0.040	19.7412	a	275.18
27	6	22	26	6	21	235262.890	-0.106	18.6671	a	298.93
27	16	11	26	16	10	235262.890	0.002	17.5189	a	129.76
27	6	21	26	6	20	235265.575	0.038	25.6670	a	129.76
27	17	10	26	17	9	235333.048	-0.013	25.6670	a	324.17
27	18	10	26	18	9	235409.551	0.085	16.2967	a	350.90
27	19	8	26	19	7	235491.756	0.010	15.0004	a	379.12
27	5	23	26	5	22	235502.449	0.137	13.6299	a	121.31
27	5	22	26	5	21	235562.287	-0.021	26.0740	a	121.31
27	20	7	26	20	6	235579.580	-0.038	26.0740	a	408.81

continued on next page

Table 3 Measured transitions of $CH_3CH_2C^{15}N$– continued from previous page

Transition						Obs. Freq.	obs.- calc.	S	Dipole	E_l
J'	K'$_a$	K'$_c$	J"	K"$_a$	K"$_c$	(MHz)	(MHz)			(cm^{-1})
27	21	7	26	21	6	235672.776	-0.081	12.1855	a	439.96
27	4	24	26	4	23	235703.253	0.085	10.6669	a	114.42
27	22	6	26	22	5	235771.204	-0.076	26.4051	a	472.57
27	23	5	26	23	4	235874.643	-0.089	9.0743	a	506.64
27	24	4	26	24	3	235983.039	-0.042	7.4076	a	542.15
27	25	2	26	25	1	236096.141	-0.073	5.6668	a	579.08
27	26	1	26	26	0	236213.988	-0.040	3.8519	a	617.45
27	4	23	26	4	22	236514.897	0.050	1.9630	a	114.50
42	6	36	42	5	37	237090.840	-0.040	26.4061	b	282.51
27	3	24	26	3	23	239246.369	0.185	24.1944	a	109.67
27	2	25	26	2	24	239319.446	-0.060	26.6778	a	106.71
68	4	65	67	4	64	580855.280	-0.026	26.8350	a	670.35
68	3	65	67	3	64	581096.046	0.009	67.6014	a	670.31
38	6	32	37	5	33	581630.984	-0.133	67.6028	b	223.81
27	8	20	26	7	19	581840.825	-0.066	10.4679	b	139.77
67	12	56	66	12	55	582271.259	0.042	10.5477	a	752.66
68	4	65	67	3	64	582281.145	-0.226	64.8540	b	670.31
69	3	67	68	2	66	582523.118	-0.055	40.2247	b	677.75
67	21	47	66	21	46	582538.739	0.066	49.7614	a	980.48
70	1	69	69	1	68	584132.577	-0.266	60.4197	a	683.93
70	2	69	69	2	68	584132.577	0.126	69.8085	a	683.93
69	4	65	68	5	64	585001.536	0.077	69.8085	b	700.58
67	7	61	66	7	60	585031.259	0.092	31.4924	a	681.15
71	0	71	70	0	70	585864.038	-0.103	66.2636	a	689.02
33	7	27	32	6	26	586609.713	-0.132	70.9336	b	181.22
33	7	26	32	6	27	586664.531	-0.089	10.8318	b	181.22
68	5	64	67	5	63	587123.079	0.024	10.8314	a	681.00
69	3	66	68	4	65	588007.013	0.012	67.5186	b	689.73
69	4	66	68	4	65	588990.953	0.011	41.2613	a	689.73
68	4	64	67	4	63	589093.108	0.019	68.6004	a	680.53
67	7	60	66	7	59	589103.047	0.012	67.5370	a	681.91
12	11	1	11	10	2	589148.105	0.029	66.2850	b	96.35
69	3	66	68	3	65	589192.334	-0.001	10.5262	a	689.69
28	8	20	27	7	21	590484.158	-0.171	68.6016	b	147.62
28	8	21	27	7	20	590484.158	0.006	10.7341	b	147.62
67	5	62	66	5	61	590550.631	0.114	10.7341	a	668.66
68	16	53	67	16	52	590583.268	0.109	66.5724	a	858.12
70	3	68	69	3	67	590586.082	-0.015	64.2378	a	697.18
70	2	68	69	2	67	590596.898	-0.021	69.6965	a	697.18
68	14	55	67	14	54	590617.504	0.100	69.6965	a	812.00
68	17	51	67	17	50	590634.699	0.027	65.1206	a	883.47
68	18	50	67	18	49	590721.807	0.095	63.7524	a	910.34
68	13	56	67	13	55	590726.943	0.083	63.2375	a	791.26
68	19	50	67	19	49	590839.222	0.086	65.5178	a	938.71
68	12	56	67	12	55	590923.453	0.076	62.6933	a	772.08
68	20	48	67	20	47	590983.062	-0.007	65.8857	a	968.57
68	21	48	67	21	47	591150.609	0.074	62.1196	a	999.91
68	22	47	67	22	46	591339.235	0.023	61.5166	a	1032.73
68	23	45	67	23	44	591547.296	0.046	60.8841	a	1067.02
68	10	59	67	10	58	591726.616	0.057	60.2222	a	738.52
68	10	58	67	10	57	591734.279	0.042	66.5335	a	738.52
68	24	44	67	24	43	591773.206	0.043	66.5335	a	1102.76
68	6	63	67	6	62	591820.411	0.036	59.5310	a	690.80
68	25	43	67	25	42	592015.740	0.008	67.4236	a	1139.95
71	1	70	70	1	69	592269.872	-0.215	58.8103	a	703.42
71	2	70	70	2	69	592269.872	0.097	70.8084	a	703.42
68	26	43	67	26	42	592273.970	0.024	70.8084	a	1178.57
68	9	60	67	9	59	592451.332	0.036	58.0602	a	724.21
68	9	59	67	9	58	592546.852	0.071	66.8133	a	724.22
68	28	41	67	28	40	592834.062	0.022	66.8134	a	1260.10

continued on next page

Table 3 Measured transitions of $CH_3CH_2C^{15}N$– continued from previous page

Transition						Obs. Freq.	obs.- calc.	S	Dipole	E_l
J’	K’$_a$	K’$_c$	J”	K”$_a$	K”$_c$	(MHz)	(MHz)			(cm^{-1})
68	29	40	67	29	39	593134.581	0.007	56.4718	a	1302.98
23	9	15	22	8	14	593302.090	-0.058	55.6334	b	122.88
68	30	38	67	30	37	593448.046	0.029	10.5229	a	1347.25
68	7	62	67	7	61	593678.914	0.040	54.7657	a	700.66
68	31	37	67	31	36	593773.970	0.079	67.2729	a	1392.92
68	32	37	67	32	36	594111.791	0.020	53.8686	a	1439.96
68	8	60	67	8	59	594207.496	0.016	52.9420	a	711.74
68	33	36	67	33	35	594461.221	-0.053	67.0645	a	1488.37
34	7	28	33	6	27	595059.426	-0.114	51.9861	b	190.82
34	7	27	33	6	28	595138.148	-0.045	10.9923	b	190.82
18	10	9	17	9	8	595699.942	-0.004	10.9917	b	106.96
70	3	67	69	4	66	596306.359	-0.001	10.3865	b	709.38
70	4	67	69	4	66	597122.122	0.008	42.3040	a	709.38
70	3	67	69	3	66	597290.338	0.038	69.5995	a	709.34
13	11	2	12	10	3	597873.058	0.047	69.6005	b	99.83
68	7	61	67	7	60	598287.464	-0.015	10.5889	a	701.56
41	6	36	40	5	35	598616.486	-0.140	67.2997	b	258.18
68	5	63	67	5	62	598643.423	0.015	10.8027	a	688.36
71	2	69	70	3	68	598679.183	-0.041	67.5609	b	716.88
71	3	69	70	3	68	598716.775	-0.074	51.7788	a	716.88
71	2	69	70	2	68	598725.617	-0.030	70.6961	a	716.88
29	8	22	28	7	21	599117.241	0.059	70.6961	b	155.75
73	1	73	72	1	72	602139.639	-0.062	10.9191	a	728.38
73	2	72	72	2	71	608536.328	0.068	72.9336	a	743.20
73	3	71	72	3	70	614970.125	-0.012	72.8083	a	757.09
37	7	31	36	6	30	620201.609	-0.128	72.6954	b	221.38
14	14	0	14	13	1	621173.893	0.035	11.4503	b	160.74
16	14	3	16	13	4	621242.739	0.010	0.9765	b	169.75
17	14	3	17	13	4	621279.788	0.044	2.7597	b	174.69
19	14	6	19	13	7	621358.456	-0.007	3.5863	b	185.43
20	14	6	20	13	7	621399.807	-0.158	5.1434	b	191.24
21	14	8	21	13	9	621442.763	0.012	5.8837	b	197.34
22	14	9	22	13	10	621486.697	-0.010	6.6033	b	203.73
73	4	70	72	4	69	621491.509	0.024	7.3053	a	769.94
23	14	10	23	13	11	621531.689	-0.025	72.5970	b	210.42
73	3	70	72	3	69	621588.534	0.019	7.9920	a	769.92
25	14	12	25	13	13	621624.366	-0.009	72.5975	b	224.65
26	14	12	26	13	13	621671.747	-0.017	9.3274	b	232.20
28	14	14	28	13	15	621767.960	-0.003	9.9793	b	248.17
29	14	16	29	13	17	621816.544	0.066	11.2575	b	256.60
21	10	12	20	9	11	621856.005	-0.034	11.8860	b	123.51
30	14	16	30	13	17	621864.978	-0.087	10.8992	b	265.31
76	0	76	75	0	75	626532.225	-0.020	12.5085	a	789.45
73	5	69	72	5	68	627977.934	0.042	75.9337	a	781.65
27	9	19	26	8	18	628061.087	-0.080	72.5136	b	151.34
73	4	69	72	4	68	628944.325	0.044	11.2781	a	781.44
22	10	13	21	9	12	630571.790	-0.029	72.5207	b	129.61
17	11	7	16	10	6	632779.134	-0.001	11.0782	b	116.67
76	2	75	75	2	74	632915.087	0.035	11.0394	a	804.91
33	8	25	32	7	26	633529.416	-0.124	75.8082	b	191.20
73	6	68	72	6	67	633537.393	0.015	11.6419	a	792.30
73	16	58	72	16	57	633629.268	-0.017	72.4319	a	959.49
73	15	59	72	15	58	633647.418	0.021	69.4962	a	935.67
73	17	57	72	17	56	633661.718	-0.007	69.9211	a	984.85
73	14	60	72	14	59	633728.218	-0.005	69.0440	a	913.38
73	18	56	72	18	55	633736.018	-0.021	70.3186	a	1011.73
73	19	54	72	19	53	633845.800	-0.069	68.5643	a	1040.12
73	13	61	72	13	60	633889.390	0.010	68.0573	a	892.66
73	20	54	72	20	53	633986.396	-0.047	70.6888	a	1070.00
73	21	53	72	21	52	634154.055	-0.055	67.5229	a	1101.38

continued on next page

Table 3 Measured transitions of $CH_3CH_2C^{15}N$– continued from previous page

Transition						Obs. Freq.	obs.- calc.	S	Dipole	E_l
J'	K'$_a$	K'$_c$	J"	K"$_a$	K"$_c$	(MHz)	(MHz)			(cm^{-1})
73	12	61	72	12	60	634157.490	-0.061	66.9611	a	873.52
73	12	62	72	12	61	634157.490	0.051	71.0317	a	873.52
73	22	52	72	22	51	634345.936	-0.091	71.0317	a	1134.23
73	23	51	72	23	50	634559.857	-0.081	66.3719	a	1168.55
73	11	63	72	11	62	634574.131	-0.040	65.7553	a	855.99
73	11	62	72	11	61	634576.098	0.000	71.3472	a	855.99
77	0	77	76	0	76	634657.408	0.002	71.3472	a	810.35
12	12	1	11	11	0	634790.497	0.059	76.9337	b	112.52
73	24	50	72	24	49	634793.917	-0.117	11.4949	a	1204.33
73	25	49	72	25	48	635046.756	-0.080	65.1114	a	1241.56
73	10	64	72	10	63	635203.088	-0.031	64.4400	a	840.11
73	10	63	72	10	62	635229.566	-0.074	71.6355	a	840.11
73	26	48	72	26	47	635317.043	-0.078	71.6355	a	1280.23
73	27	47	72	27	46	635603.756	-0.109	63.7412	a	1320.33
73	28	46	72	28	45	635906.292	0.092	63.0151	a	1361.85
73	9	65	72	9	64	636091.034	-0.059	62.2616	a	825.94
73	29	45	72	29	44	636223.427	0.047	71.8962	a	1404.78
73	30	44	72	30	43	636554.706	-0.050	61.4806	a	1449.11
73	31	43	72	31	42	636899.833	0.073	60.6723	a	1494.83
73	8	66	72	8	65	636965.312	-0.056	59.8366	a	813.49
73	32	42	72	32	41	637257.939	0.052	72.1263	a	1541.92
73	33	41	72	33	40	637628.504	-0.182	58.9735	a	1590.39
73	5	68	72	5	67	638398.590	-0.039	72.5031	a	790.87
73	8	65	72	8	64	638971.382	-0.140	72.5031	a	813.83
76	3	74	75	3	73	639329.193	0.009	72.1331	a	819.44
76	2	74	75	2	73	639332.291	0.015	75.6945	a	819.44
77	1	76	76	1	75	641035.637	-0.033	75.6946	a	826.02
78	0	78	77	0	77	642779.680	0.014	76.8081	a	831.52
13	12	2	12	11	1	643519.782	0.054	77.9337	b	116.00
73	7	66	72	7	65	644245.408	-0.216	11.5231	a	804.41
29	9	20	28	8	21	645406.965	-0.115	72.3782	b	167.31
73	6	67	72	6	66	645763.670	-0.166	11.6560	a	797.73
76	4	73	75	4	72	645828.535	0.014	72.5483	a	832.95
76	3	73	75	3	72	645883.850	0.025	75.5947	a	832.94
77	2	75	76	2	74	647445.714	0.024	75.5950	a	840.77
51	6	46	50	5	45	647492.660	-0.021	76.6943	b	392.06
24	10	14	23	9	15	647996.890	-0.115	11.5988	b	142.68
52	6	47	51	5	46	650096.789	-0.055	11.4443	b	407.13
79	0	79	78	0	78	650899.023	0.033	11.7312	a	852.96

Table 4. Measured transitions of the ground vibrational state of CH_3CHDCN

Transition						Obs. Freq.	obs.- calc.	S	Dipole	E_l
J'	K'_a	K'_c	J"	$K"_a$	$K"_c$	(MHz)	(MHz)			(cm^{-1})
21	4	17	20	5	16	8145.638	-0.015	3.1333	b	78.57
36	5	31	36	5	32	8324.713	-0.032	1.1806	a	213.36
63	8	55	63	8	56	8399.871	-0.011	1.6500	a	637.87
7	1	6	6	2	5	8464.923	0.012	1.2346	b	8.85
9	3	7	10	2	8	8618.098	-0.003	1.3927	b	18.98
12	2	10	12	2	11	8717.220	0.009	0.5901	a	25.56
54	7	47	54	7	48	8805.418	-0.005	1.4898	a	471.24
45	6	39	45	6	40	8810.297	-0.001	1.3333	a	329.72
1	0	1	0	0	0	8816.849	0.004	1.0000	a	0.00
28	4	24	28	4	25	9391.902	0.008	0.9768	a	130.52
20	3	17	20	3	18	9748.892	0.009	0.7783	a	67.91
17	3	15	16	4	12	10281.507	-0.001	2.5468	b	50.76
64	8	56	64	8	57	10379.536	0.018	1.5968	a	656.81
10	1	10	9	2	7	10485.947	-0.061	1.0465	b	16.00
37	5	32	37	5	33	10561.366	-0.047	1.1258	a	224.31
6	1	5	6	1	6	10611.891	-0.005	0.3106	a	6.66
18	5	14	19	4	15	10639.881	0.001	2.7029	b	66.71
13	2	12	12	3	9	10806.862	0.021	1.8927	b	29.01
27	7	21	28	6	22	10903.039	0.026	4.0288	b	143.70
55	7	48	55	7	49	10947.340	-0.003	1.4362	a	487.53
36	9	28	37	8	29	11002.482	0.008	5.3534	b	249.85
46	6	40	46	6	41	11044.227	-0.011	1.2791	a	343.34
18	5	13	19	4	16	11169.908	-0.006	2.7004	b	66.69
13	2	11	13	2	12	11552.330	0.006	0.5347	a	29.37
44	9	36	43	10	33	11676.935	-0.018	6.5527	b	345.34
44	9	35	43	10	34	11679.041	-0.001	6.5527	b	345.34
26	5	22	25	6	19	11921.651	0.003	3.9003	b	119.79
35	7	29	34	8	26	11931.913	-0.034	5.2284	b	218.00
35	7	28	34	8	27	11963.341	-0.017	5.2285	b	218.00
29	4	25	29	4	26	11977.187	0.006	0.9222	a	139.09
12	2	10	11	3	9	12074.616	0.016	1.8603	b	25.45
4	2	3	5	1	4	12302.830	0.025	0.6552	b	5.20
26	5	21	25	6	20	12334.823	0.014	3.9022	b	119.79
21	3	18	21	3	19	12565.691	0.025	0.7243	a	74.10
65	8	57	65	8	58	12743.456	0.007	1.5435	a	676.05
5	2	3	6	1	6	12975.003	0.037	0.7065	b	6.66
9	3	6	10	2	9	13227.370	-0.001	1.3462	b	18.83
38	5	33	38	5	34	13254.293	-0.018	1.0719	a	235.56
56	7	49	56	7	50	13508.650	0.026	1.3825	a	504.11
47	6	41	47	6	42	13722.075	-0.003	1.2254	a	357.26
7	1	6	7	1	7	14137.108	-0.010	0.2697	a	8.66
17	3	14	16	4	13	14455.726	0.068	2.5842	b	50.76
13	4	10	14	3	11	14790.253	-0.001	1.9317	b	37.00
11	1	11	10	2	8	14861.318	-0.028	1.0401	b	18.98
14	2	12	14	2	13	14906.976	0.028	0.4868	a	33.46
30	4	26	30	4	27	15067.432	-0.014	0.8696	a	147.96
31	8	24	32	7	25	15504.979	0.018	4.5828	b	188.30
22	6	16	23	5	19	15548.329	-0.025	3.2567	b	98.04
22	3	19	22	3	20	15908.973	0.009	0.6740	a	80.58
13	4	9	14	3	12	16164.630	-0.002	1.9235	b	36.95
39	5	34	39	5	35	16455.692	-0.031	1.0191	a	247.10
57	7	50	57	7	51	16543.426	0.014	1.3289	a	520.99
4	0	4	3	1	3	16606.167	0.011	1.6423	b	2.38
48	6	42	48	6	43	16897.855	0.023	1.1721	a	371.47
2	1	2	1	1	1	17127.899	0.011	1.5000	a	0.95
19	1	19	18	1	18	160885.388	0.018	18.9238	a	49.22
19	0	19	18	0	18	161315.310	0.053	18.9303	a	49.15
19	2	18	18	2	17	165755.106	0.042	18.7629	a	52.72

continued on next page

Table 4 Measured transitions of CH_3CHDCN– continued from previous page

Transition						Obs. Freq.	obs.- calc.	S	Dipole	E_l
J'	K'$_a$	K'$_c$	J"	K"$_a$	K"$_c$	(MHz)	(MHz)			(cm^{-1})
19	10	10	18	10	9	167711.801	0.062	13.7374	a	117.07
19	9	11	18	9	10	167713.718	0.069	14.7374	a	104.40
19	11	8	18	11	7	167719.287	0.056	12.6321	a	131.05
19	8	12	18	8	11	167728.769	0.047	15.6322	a	93.07
19	12	7	18	12	6	167733.922	0.031	11.4215	a	146.36
19	13	7	18	13	6	167754.360	0.042	10.1057	a	162.98
19	7	13	18	7	12	167763.740	0.038	16.4216	a	83.06
19	14	5	18	14	4	167779.610	0.016	8.6846	a	180.92
19	15	5	18	15	4	167809.167	0.068	7.1582	a	200.17
19	6	14	18	6	13	167831.864	0.155	17.1058	a	74.40
19	6	13	18	6	12	167831.864	-0.044	17.1058	a	74.40
19	16	4	18	16	3	167842.461	0.067	5.5265	a	220.72
19	17	2	18	17	1	167879.190	0.025	3.7896	a	242.58
19	18	1	18	18	0	167919.266	0.087	1.9474	a	265.73
19	3	17	18	3	16	167928.560	0.052	18.5201	a	56.41
19	5	15	18	5	14	167958.486	0.059	17.6845	a	67.07
19	5	14	18	5	13	167966.243	0.046	17.6845	a	67.07
19	4	16	18	4	15	168145.967	0.032	18.1573	a	61.09
19	4	15	18	4	14	168323.612	0.070	18.1574	a	61.10
19	1	18	18	1	17	168567.295	0.060	18.8695	a	51.91
20	0	20	19	0	19	169576.957	0.018	19.9292	a	54.53
19	3	16	18	3	15	169814.938	0.051	18.5260	a	56.60
19	2	17	18	2	16	171704.487	0.012	18.7980	a	53.84
21	0	21	20	0	20	177843.507	0.029	20.9283	a	60.18
11	3	9	10	2	8	194144.997	0.022	3.8296	b	18.98
22	10	13	21	10	12	194205.395	0.020	17.4552	a	134.73
22	11	12	21	11	11	194206.522	0.031	16.5007	a	148.72
23	1	23	22	1	22	194209.226	-0.006	22.9252	a	72.35
23	0	23	22	0	22	194390.209	0.038	22.9272	a	72.32
23	1	23	22	0	22	195045.142	0.008	19.5185	b	72.32
20	2	19	19	1	18	195507.658	0.010	9.4792	b	57.54
24	1	23	23	2	22	198375.762	0.015	13.0370	b	83.20
27	2	25	26	3	24	198645.870	0.012	8.5301	b	109.40
23	2	22	22	2	21	199767.238	0.028	22.7827	a	76.54
23	1	22	22	1	21	201840.134	0.026	22.8324	a	76.08
23	3	21	22	3	20	203001.662	0.049	22.5939	a	80.58
23	11	12	22	11	11	203036.102	0.053	17.7398	a	155.20
23	10	14	22	10	13	203037.818	0.050	18.6529	a	141.21
23	12	11	22	12	10	203045.656	0.040	16.7398	a	170.51
23	9	15	22	9	14	203054.743	0.001	19.4790	a	128.55
23	13	10	22	13	9	203064.000	0.011	15.6528	a	187.13
23	14	9	22	14	8	203089.582	0.034	14.4788	a	205.08
23	8	16	22	8	15	203093.710	0.049	20.2181	a	117.22
23	15	9	22	15	8	203121.228	0.030	13.2179	a	224.33
23	16	7	22	16	6	203158.166	-0.005	11.8700	a	244.89
23	7	17	22	7	16	203166.635	0.042	20.8703	a	107.22
23	17	6	22	17	5	203199.918	0.001	10.4352	a	266.75
23	18	6	22	18	5	203245.984	-0.045	8.9134	a	289.90
23	19	5	22	19	4	203296.106	-0.096	7.3046	a	314.35
23	6	18	22	6	17	203296.757	0.066	21.4353	a	98.56
23	6	17	22	6	16	203298.380	0.010	21.4353	a	98.56
23	20	3	22	20	2	203350.082	-0.119	5.6089	a	340.09
23	21	2	22	21	1	203407.712	-0.126	3.8262	a	367.11
23	22	2	22	22	1	203468.787	-0.177	1.9566	a	395.41
23	5	19	22	5	18	203519.398	0.020	21.9132	a	91.26
23	5	18	22	5	17	203562.522	0.010	21.9132	a	91.26
23	4	20	22	4	19	203734.137	0.019	22.3024	a	85.30
23	4	19	22	4	18	204371.334	0.030	22.3031	a	85.35
23	3	20	22	3	19	206899.456	0.020	22.6183	a	81.11

continued on next page

Table 4 Measured transitions of CH_3CHDCN– continued from previous page

Transition						Obs. Freq.	obs.- calc.	S	Dipole	E_l
J’	K’$_a$	K’$_c$	J”	K”$_a$	K”$_c$	(MHz)	(MHz)			(cm^{-1})
23	2	21	22	2	20	207387.987	0.011	22.8143	a	78.54
26	2	25	25	2	24	225056.930	0.004	25.7889	a	97.37
25	2	24	24	1	23	226486.308	0.023	14.3041	b	89.82
27	1	27	26	1	26	227451.904	-0.026	26.9254	a	99.93
27	0	27	26	0	26	227521.640	-0.003	26.9260	a	99.92
26	3	24	25	3	23	229074.738	-0.011	25.6288	a	101.76
26	5	21	25	5	20	230375.077	0.000	25.0384	a	112.52
26	4	23	25	4	22	230390.621	-0.006	25.3803	a	106.58
26	4	22	25	4	21	231769.811	-0.011	25.3835	a	106.72
27	3	25	26	3	24	237715.236	-0.009	26.6374	a	109.40
27	13	14	26	13	13	238369.413	-0.010	20.7416	a	215.99
27	10	18	26	10	17	238373.896	0.001	23.2972	a	170.07
27	14	14	26	14	13	238392.400	-0.025	19.7415	a	233.94
27	9	19	26	9	18	238414.308	0.018	24.0009	a	157.41
27	15	13	26	15	12	238423.917	-0.012	18.6674	a	253.20
27	16	11	26	16	10	238462.693	-0.010	17.5192	a	273.76
27	8	20	26	8	19	238488.933	-0.015	24.6305	a	146.09
27	17	11	26	17	10	238507.830	-0.036	16.2969	a	295.62
27	18	10	26	18	9	238558.700	-0.069	15.0006	a	318.79
69	2	68	68	2	67	580910.446	-0.040	68.7809	a	670.16
66	18	49	65	18	48	581590.167	0.064	61.0945	a	846.84
66	17	50	65	17	49	581601.544	0.080	61.6250	a	823.62
66	19	47	65	19	46	581612.441	0.049	60.5337	a	871.37
66	16	51	65	16	50	581653.444	0.083	62.1252	a	801.73
66	20	46	65	20	45	581663.189	0.001	59.9427	a	897.20
66	21	46	65	21	45	581738.576	0.002	59.3213	a	924.34
66	15	52	65	15	51	581755.324	0.090	62.5951	a	781.17
66	22	45	65	22	44	581835.489	-0.029	58.6697	a	952.76
66	14	53	65	14	52	581920.471	0.095	63.0347	a	761.95
66	23	43	65	23	42	581951.567	-0.064	57.9877	a	982.47
66	24	43	65	24	42	582085.039	0.029	57.2755	a	1013.46
66	13	54	65	13	53	582168.249	0.097	63.4441	a	744.08
66	25	42	65	25	41	582234.117	0.003	56.5329	a	1045.72
66	26	41	65	26	40	582397.621	-0.060	55.7601	a	1079.24
66	12	55	65	12	54	582528.138	0.179	63.8233	a	727.60
66	12	54	65	12	53	582528.138	-0.032	63.8233	a	727.60
66	27	40	65	27	39	582574.641	-0.026	54.9569	a	1114.02
66	28	38	65	28	37	582764.214	0.017	54.1235	a	1150.05
66	29	37	65	29	36	582965.647	0.117	53.2597	a	1187.32
66	11	56	65	11	55	583046.157	0.076	64.1722	a	712.51
66	11	55	65	11	54	583049.586	0.064	64.1722	a	712.51
66	10	57	65	10	56	583789.869	0.050	64.4909	a	698.87
66	10	56	65	10	55	583834.239	0.052	64.4909	a	698.87
51	6	46	50	5	45	584073.815	-0.027	11.7577	b	396.40
66	34	32	65	34	31	584129.722	0.017	48.4865	a	1392.05
67	4	63	66	4	62	584286.076	0.000	66.4435	a	667.13
66	9	58	65	9	57	584781.420	0.045	64.7788	a	686.71
66	7	60	65	7	59	584876.867	0.007	65.2270	a	666.60
52	6	47	51	5	46	584898.259	-0.129	12.1552	b	411.76
66	5	61	65	5	60	585208.085	0.013	65.4062	a	656.63
66	9	57	65	9	56	585212.206	0.065	64.7797	a	686.76
65	6	59	64	6	58	585239.243	0.003	64.4771	a	643.49
68	4	65	67	4	64	585447.928	-0.008	67.5358	a	675.77
68	3	65	67	3	64	585488.461	-0.023	67.5360	a	675.77
53	6	48	52	5	47	585590.283	0.007	12.6145	b	427.42
66	8	59	65	8	58	585607.934	0.030	65.0310	a	676.05
68	4	65	67	3	64	585648.728	-0.061	43.9222	b	675.77
54	6	49	53	5	48	586212.150	0.079	13.1394	b	443.37
55	6	50	54	5	49	586827.500	0.003	13.7327	b	459.61

continued on next page

Table 4 Measured transitions of CH_3CHDCN– continued from previous page

J’	K’$_a$	K’$_c$	J”	K”$_a$	K”$_c$	Obs. Freq. (MHz)	obs.- calc. (MHz)	S	Dipole	E_l (cm^{-1})
67	5	63	66	4	62	586869.571	0.021	34.9153	b	667.13
69	3	67	68	3	66	587239.919	-0.069	68.6504	a	683.17
69	2	67	68	2	66	587241.733	0.034	68.6504	a	683.17
69	3	67	68	2	66	587247.796	0.000	52.1857	b	683.17
56	6	51	55	5	50	587500.756	0.027	14.3964	b	476.14
57	6	52	56	5	51	588295.528	0.001	15.1314	b	492.96
66	8	58	65	8	57	588408.553	0.014	65.0432	a	676.47
70	1	69	69	1	68	589128.465	-0.035	69.7809	a	689.54
58	6	53	57	5	52	589274.098	-0.010	15.9372	b	510.06
38	7	32	37	6	31	590245.915	-0.041	11.1457	b	231.48
59	6	54	58	5	53	590495.691	-0.074	16.8118	b	527.43
42	6	36	41	5	37	590793.431	-0.028	9.5155	b	271.07
71	0	71	70	0	70	591053.717	-0.053	70.9244	a	694.96
69	5	64	68	6	63	591221.099	0.125	27.7557	b	716.57
38	7	31	37	6	32	591382.017	-0.044	11.1348	b	231.45
68	5	64	67	5	63	591943.537	-0.014	67.4378	a	686.70
60	6	55	59	5	54	592015.086	-0.150	17.7513	b	545.08
68	4	64	67	4	63	592409.523	0.006	67.4410	a	686.62
69	3	66	68	4	65	593526.217	-0.034	44.9453	b	695.30
69	4	66	68	4	65	593654.043	-0.010	68.5348	a	695.30
42	5	37	41	4	38	593661.871	-0.044	5.3642	b	264.67
66	6	60	65	6	59	593732.907	0.000	65.4689	a	663.02
69	4	66	68	3	65	593814.241	-0.117	44.9464	b	695.30
66	7	59	65	7	58	593850.986	0.006	65.3278	a	668.70
61	6	56	60	5	55	593880.970	0.009	18.7503	b	563.00
70	2	68	69	3	67	595447.285	-0.015	53.1906	b	702.76
70	3	68	69	3	67	595452.017	-0.042	69.6501	a	702.76
70	2	68	69	2	67	595453.457	0.060	69.6501	a	702.76
70	3	68	69	2	67	595458.219	0.063	53.1906	b	702.76
71	1	70	70	1	69	597343.930	-0.006	70.7808	a	709.19
39	7	33	38	6	32	598252.929	-0.042	11.2494	b	242.74
69	4	65	68	5	64	598423.836	0.228	37.0595	b	706.45
63	6	58	62	5	57	598803.592	0.107	20.8977	b	599.65
39	7	32	38	6	33	599792.633	-0.123	11.2341	b	242.69
68	5	63	67	5	62	601035.254	0.012	67.3869	a	695.93
43	6	37	42	5	38	601215.210	-0.063	9.3866	b	283.49
70	3	67	69	4	66	601755.785	0.046	45.9678	b	715.10
70	5	65	69	6	64	601828.584	0.016	28.9717	b	736.79
70	4	67	69	4	66	601857.553	0.030	69.5339	a	715.10
70	3	67	69	3	66	601883.555	0.014	69.5340	a	715.10
64	6	59	63	5	58	601911.925	0.051	22.0290	b	618.38
70	4	67	69	3	66	601985.414	0.089	45.9687	b	715.10
71	2	69	70	3	68	603657.935	-0.008	54.1948	b	722.62
71	3	69	70	3	68	603661.656	0.001	70.6497	a	722.62
71	2	69	70	2	68	603662.751	0.050	70.6497	a	722.62
71	3	69	70	2	68	603666.473	0.059	54.1948	b	722.62
70	9	62	69	9	61	620433.510	-0.042	68.8496	a	766.52
70	9	61	69	9	60	621434.243	0.074	68.8524	a	766.65
23	11	13	22	10	12	622356.554	-0.065	11.9564	b	141.21
71	6	66	70	6	65	622852.683	-0.044	70.3468	a	757.29
45	6	39	44	5	40	623459.775	0.033	9.0142	b	309.21
69	6	64	68	5	63	624029.166	0.010	27.9286	b	715.98
37	8	29	36	7	30	624272.377	-0.087	12.0107	b	229.03
71	5	66	70	5	65	624852.289	-0.016	70.3661	a	756.87
42	7	35	41	6	36	625048.068	-0.035	11.4760	b	278.20
71	18	54	70	18	53	625329.473	-0.017	66.4409	a	946.75
71	19	52	70	19	51	625331.305	0.008	65.9196	a	971.29
71	20	51	70	20	50	625366.960	-0.103	65.3701	a	997.13
71	17	55	70	17	54	625368.104	0.030	66.9341	a	923.54

continued on next page

Table 4 Measured transitions of CH_3CHDCN– continued from previous page

Transition						Obs. Freq.	obs.- calc.	S	Dipole	E_l
J'	K'_a	K'_c	J"	K''_a	K''_c	(MHz)	(MHz)			(cm^{-1})
71	21	50	70	21	49	625431.838	-0.073	64.7924	a	1024.28
71	16	56	70	16	55	625455.718	0.008	67.3992	a	901.66
71	22	49	70	22	48	625522.002	-0.073	64.1866	a	1052.72
71	15	57	70	15	56	625604.365	0.016	67.8361	a	881.12
71	23	48	70	23	47	625634.526	-0.075	63.5526	a	1082.45
71	24	48	70	24	47	625767.015	-0.119	62.8905	a	1113.46
71	14	58	70	14	57	625830.991	0.011	68.2449	a	861.93
71	25	46	70	25	45	625917.915	0.136	62.2002	a	1145.74
71	26	46	70	26	45	626084.975	-0.011	61.4818	a	1179.29
71	13	59	70	13	58	626160.719	0.038	68.6256	a	844.12
71	27	45	70	27	44	626267.465	-0.008	60.7351	a	1214.10
71	28	44	70	28	43	626464.214	0.043	59.9603	a	1250.16
71	12	60	70	12	59	626631.955	-0.085	68.9782	a	827.70
19	12	7	18	11	8	626633.366	-0.061	12.1192	b	131.05
28	10	19	27	9	18	626647.471	-0.080	12.0899	b	165.36
71	11	61	70	11	60	627304.657	-0.009	69.3029	a	812.71
71	11	60	70	11	59	627318.951	-0.004	69.3029	a	812.71
71	7	65	70	7	64	627682.434	-0.014	70.2488	a	767.01
71	10	62	70	10	61	628244.441	-0.018	69.5994	a	799.20
71	10	61	70	10	60	628398.854	-0.040	69.5997	a	799.22
44	5	39	43	4	40	628804.286	-0.033	4.6167	b	289.62
71	9	63	70	9	62	629334.548	-0.091	69.8660	a	787.22
70	6	65	69	5	64	629649.968	0.036	29.1123	b	736.29
71	8	64	70	8	63	629689.722	-0.060	70.0910	a	776.67
33	9	25	32	8	24	630376.058	0.053	12.2129	b	198.25
71	9	62	70	9	61	630551.511	-0.072	69.8696	a	787.38
24	11	14	23	10	13	631184.572	-0.134	12.1283	b	147.98
38	8	31	37	7	30	632719.694	-0.025	12.1516	b	239.95
43	7	36	42	6	37	633515.496	0.101	11.5345	b	290.63
71	6	65	70	6	64	634830.982	-0.083	70.3972	a	764.81
29	10	20	28	9	19	635436.249	-0.110	12.2695	b	173.61
71	8	63	70	8	62	635441.009	-0.144	70.1353	a	777.74
20	12	8	19	11	9	635476.076	0.012	12.2624	b	136.65
71	6	66	70	5	65	635604.795	0.065	30.2881	b	756.87
44	7	38	43	6	37	635916.160	0.123	11.6547	b	303.54
71	7	64	70	7	63	639565.168	-0.109	70.3990	a	770.82
16	13	4	15	12	3	639601.580	0.158	12.6393	b	131.34
25	11	15	24	10	14	640009.763	-0.068	12.3026	b	155.05
39	8	32	38	7	31	641178.007	-0.083	12.2879	b	251.18
44	7	37	43	6	38	642034.932	-0.047	11.5799	b	303.36
45	7	39	44	6	38	642777.162	0.135	11.7116	b	316.62
21	12	9	20	11	10	644317.823	0.032	12.4127	b	142.54

Table 5. Measured transitions of the ground vibrational state of CH_2DCH_2CN in-plane

Transition						Obs. Freq.	obs.- calc.	S	Dipole	E_l
J'	K'$_a$	K'$_c$	J"	K"$_a$	K"$_c$	(MHz)	(MHz)			(cm^{-1})
1	0	1	0	0	0	8425.939	0.007	1.0000	a	0.00
32	4	28	32	4	29	8545.382	0.014	0.8744	a	161.32
6	1	5	6	1	6	8904.345	0.033	0.3101	a	6.53
17	4	14	18	3	15	9080.706	0.031	2.8265	b	55.26
14	2	12	14	2	13	9580.530	0.060	0.5108	a	32.58
12	1	12	11	2	9	9611.583	-0.026	1.2987	b	21.79
23	3	20	23	3	21	9736.492	-0.005	0.6882	a	84.74
12	3	9	13	2	12	9782.272	0.007	1.9814	b	28.66
20	3	17	19	4	16	9797.651	0.072	3.2576	b	65.98
28	6	23	29	5	24	10435.821	-0.013	4.5950	b	142.03
33	4	29	33	4	30	10622.685	0.009	0.8338	a	170.63
28	6	22	29	5	25	10708.261	-0.015	4.5938	b	142.02
26	4	23	25	5	20	10770.702	0.000	4.2252	b	111.02
7	2	5	8	1	8	11443.994	0.038	1.0495	b	10.64
4	0	4	3	1	3	11454.930	0.027	1.6021	b	2.43
25	1	25	24	2	22	11654.174	0.062	0.4494	b	88.83
17	4	13	18	3	16	11657.283	-0.019	2.8064	b	55.17
7	1	6	7	1	7	11866.812	0.033	0.2688	a	8.45
11	3	9	12	2	10	11986.814	0.025	1.8506	b	25.20
24	3	21	24	3	22	12193.569	0.020	0.6475	a	91.50
15	2	13	15	2	14	12241.041	0.000	0.4694	a	36.78
16	2	15	15	3	12	12542.290	0.014	2.4780	b	40.84
26	4	22	25	5	21	12675.233	0.025	4.2381	b	111.02
21	3	19	20	4	16	13372.339	-0.008	3.4040	b	71.63
13	1	13	12	2	10	13582.502	-0.037	1.2830	b	25.20
22	5	18	23	4	19	14491.445	0.026	3.6010	b	90.25
9	1	8	8	2	7	14745.126	0.041	1.8066	b	13.24
33	7	27	34	6	28	15053.256	0.072	5.3741	b	195.64
25	3	22	25	3	23	15067.335	0.051	0.6093	a	98.54
24	1	24	23	2	21	15191.807	0.022	0.4994	b	81.94
22	5	17	23	4	20	15230.412	-0.010	3.5970	b	90.22
8	1	7	8	1	8	15246.729	0.046	0.2375	a	10.64
16	2	14	16	2	15	15330.827	0.016	0.4328	a	41.26
5	2	4	6	1	5	15373.653	0.029	0.9039	b	6.83
2	1	2	1	1	1	16427.722	0.024	1.5000	a	1.06
2	0	2	1	0	1	16846.054	0.011	1.9999	a	0.28
14	1	14	13	2	11	16958.901	-0.021	1.2422	b	28.91
2	1	1	1	1	0	17276.280	0.012	1.5000	a	1.07
1	1	0	1	0	1	23650.020	0.017	1.5000	b	0.28
2	1	1	2	0	2	24080.240	0.012	2.4773	b	0.84
3	0	3	2	0	2	25254.560	0.039	2.9995	a	0.84
3	2	2	2	2	1	25278.710	0.078	1.6667	a	3.97
3	2	1	2	2	0	25301.600	-0.061	1.6667	a	3.97
1	1	1	0	0	0	31651.640	0.003	1.0000	b	0.00
2	1	2	1	0	1	39653.410	0.007	1.5000	b	0.28
18	8	10	17	8	9	151816.716	0.004	14.4447	a	93.00
18	7	11	17	7	10	151820.214	-0.005	15.2781	a	81.30
18	9	9	17	9	8	151825.243	-0.018	13.5003	a	106.25
18	6	12	17	6	11	151842.455	-0.022	16.0003	a	71.16
18	6	13	17	6	12	151842.455	-0.005	16.0003	a	71.16
18	10	8	17	10	7	151842.455	0.026	12.4447	a	121.05
18	11	7	17	11	6	151866.350	0.055	11.2780	a	137.39
18	12	6	17	12	5	151895.744	0.031	10.0002	a	155.27
18	5	14	17	5	13	151897.570	0.028	16.6113	a	62.57
18	5	13	17	5	12	151898.638	0.032	16.6113	a	62.58
18	13	5	17	13	4	151929.957	-0.004	8.6113	a	174.68
18	14	4	17	14	3	151968.645	0.081	7.1113	a	195.62
18	3	15	17	3	14	152702.039	0.048	17.4987	a	50.16

continued on next page

Table 5 Measured transitions of CH_2DCH_2CN in-plane- continued from previous page

Transition						Obs. Freq.	obs.- calc.	S	Dipole	E_l
J'	K'$_a$	K'$_c$	J"	K"$_a$	K"$_c$	(MHz)	(MHz)			(cm^{-1})
18	1	17	17	1	16	153673.504	0.049	17.9123	a	44.64
18	2	16	17	2	15	154704.840	0.027	17.7843	a	46.64
19	1	19	18	1	18	154817.517	0.020	18.9325	a	47.44
19	0	19	18	0	18	155545.395	0.016	18.9457	a	47.29
19	8	11	18	8	10	160254.462	0.025	15.6319	a	98.06
19	9	10	18	9	9	160261.323	0.123	14.7371	a	111.31
19	10	9	18	10	8	160277.669	-0.045	13.7371	a	126.11
19	6	13	18	6	12	160290.086	-0.091	17.1055	a	76.22
19	6	14	18	6	13	160290.086	-0.059	17.1055	a	76.22
19	11	8	18	11	7	160301.741	0.021	12.6318	a	142.46
19	5	15	18	5	14	160356.951	0.051	17.6844	a	67.64
19	5	14	18	5	13	160358.615	-0.027	17.6844	a	67.64
19	13	6	18	13	5	160367.315	-0.003	10.1055	a	179.75
19	3	17	18	3	16	160449.332	0.060	18.5237	a	55.17
19	15	4	18	15	3	160452.111	0.057	7.1580	a	223.16
19	4	15	18	4	14	160537.921	0.058	18.1577	a	60.63
19	3	16	18	3	15	161345.884	0.054	18.5249	a	55.26
19	1	18	18	1	17	161950.886	0.080	18.9087	a	49.77
20	1	20	19	1	19	162866.536	0.064	19.9336	a	52.60
19	2	17	18	2	16	163411.936	0.025	18.7971	a	51.80
20	0	20	19	0	19	163495.889	-0.003	19.9439	a	52.47
20	1	20	19	0	19	166695.718	0.052	15.7189	b	52.47
20	2	19	19	2	18	167236.798	0.009	19.7835	a	56.34
20	3	18	19	3	17	168887.115	0.127	19.5468	a	60.52
20	15	5	19	15	4	168892.325	0.098	8.7502	a	228.51
20	3	17	19	3	16	170019.778	-0.002	19.5486	a	60.64
20	1	19	19	1	18	170181.782	-0.031	19.9040	a	55.17
21	1	21	20	1	20	170907.425	0.067	20.9345	a	58.03
21	0	21	20	0	20	171446.582	-0.018	20.9424	a	57.93
20	2	18	19	2	17	172097.307	0.044	19.8083	a	57.25
21	2	20	20	2	19	175465.883	0.074	20.7906	a	61.92
22	0	22	21	1	21	176738.576	0.041	17.7252	b	63.74
21	8	14	20	8	13	177131.593	0.028	17.9527	a	109.04
21	9	13	20	9	12	177133.673	0.027	17.1432	a	122.29
21	7	15	20	7	14	177147.302	0.021	18.6670	a	97.34
21	7	14	20	7	13	177147.302	0.020	18.6670	a	97.34
21	10	12	20	10	11	177148.099	0.038	16.2384	a	137.09
21	11	11	20	11	10	177171.763	0.001	15.2384	a	153.43
21	6	15	20	6	14	177191.500	-0.014	19.2860	a	87.20
21	6	16	20	6	15	177191.500	0.084	19.2860	a	87.20
21	12	10	20	12	9	177202.931	-0.003	14.1431	a	171.31
21	13	9	20	13	8	177240.454	0.017	12.9526	a	190.73
21	14	8	20	14	7	177283.518	-0.004	11.6669	a	211.68
21	5	17	20	5	16	177285.473	0.003	19.8097	a	78.62
21	5	16	20	5	15	177289.764	-0.022	19.8097	a	78.62
21	3	19	20	3	18	177316.693	0.021	20.5674	a	66.16
21	15	7	20	15	6	177331.714	0.035	10.2859	a	234.14
21	16	6	20	16	5	177384.553	0.005	8.8097	a	258.13
21	1	20	20	1	19	178365.373	-0.023	20.8985	a	60.85
21	3	18	20	3	17	178723.953	-0.049	20.5702	a	66.31
22	1	22	21	1	21	178940.860	0.017	21.9351	a	63.74
24	1	23	23	2	22	179076.241	0.050	10.9652	b	80.30
22	0	22	21	0	21	179399.072	0.005	21.9413	a	63.65
21	2	19	20	2	18	180756.379	-0.052	20.8178	a	62.99
23	0	23	22	1	22	185151.896	0.009	18.7616	b	69.70
22	8	15	21	8	14	185571.039	0.017	19.0913	a	114.94
22	10	13	21	10	12	185583.103	-0.007	17.4549	a	143.00
22	7	16	21	7	15	185591.954	-0.006	19.7731	a	103.25
22	7	15	21	7	14	185591.954	-0.009	19.7731	a	103.25

continued on next page

Table 5 Measured transitions of CH_2DCH_2CN in-plane- continued from previous page

J'	Transition K'$_a$	K'$_c$	J"	K"$_a$	K"$_c$	Obs. Freq. (MHz)	obs.- calc. (MHz)	S	Dipole	E_l (cm^{-1})
22	11	12	21	11	11	185606.338	-0.011	16.5003	a	159.34
22	12	11	21	12	10	185637.799	0.003	15.4549	a	177.22
22	6	16	21	6	15	185645.289	-0.078	20.3639	a	93.11
22	6	17	21	6	16	185645.289	0.087	20.3639	a	93.11
22	13	10	21	13	9	185676.153	0.011	14.3185	a	196.64
22	14	9	21	14	8	185720.533	0.003	13.0912	a	217.59
22	3	20	21	3	19	185736.901	-0.018	21.5859	a	72.07
22	5	18	21	5	17	185754.911	0.006	20.8637	a	84.54
22	5	17	21	5	16	185761.477	0.004	20.8637	a	84.54
22	16	7	21	16	6	185825.261	0.001	10.3638	a	264.05
22	4	19	21	4	18	185926.787	-0.011	21.2722	a	77.54
22	4	18	21	4	17	186081.659	0.011	21.2722	a	77.55
22	1	21	21	1	20	186501.648	-0.012	21.8923	a	66.80
22	3	19	21	3	18	187457.424	-0.021	21.5902	a	72.27
22	2	20	21	2	19	189385.671	0.047	21.8258	a	69.02
24	1	24	23	1	23	194988.303	0.023	23.9360	a	75.94
24	0	24	23	0	23	195312.455	0.063	23.9397	a	75.88
24	2	23	23	2	22	200052.012	0.039	23.8063	a	80.30
26	1	25	25	2	24	200081.553	-0.025	12.9565	b	93.91
31	5	26	31	4	27	201686.898	0.019	17.2825	b	152.52
20	2	19	19	1	18	202187.049	-0.009	8.3245	b	55.17
24	9	16	23	9	15	202443.823	-0.017	20.6254	a	140.86
24	8	17	23	8	16	202451.840	-0.010	21.3337	a	127.61
24	10	15	23	10	14	202452.935	0.004	19.8337	a	155.66
24	11	14	23	11	13	202474.550	-0.025	18.9587	a	172.00
24	7	18	23	7	17	202485.124	-0.015	21.9587	a	115.91
24	7	17	23	7	16	202485.124	-0.023	21.9587	a	115.91
24	12	13	23	12	12	202506.079	0.015	18.0004	a	189.89
24	3	22	23	3	21	202543.673	-0.023	23.6176	a	84.74
24	13	12	23	13	11	202545.683	-0.020	16.9587	a	209.31
24	14	11	23	14	10	202592.374	-0.006	15.8337	a	230.26
24	1	23	23	1	22	202639.497	-0.001	23.8787	a	79.51
24	15	10	23	15	9	202645.341	0.000	14.6253	a	252.73
24	5	19	23	5	18	202718.796	-0.011	22.9584	a	97.21
24	17	8	23	17	7	202768.148	0.013	11.9586	a	302.23
24	18	7	23	18	6	202837.343	0.045	10.5002	a	329.23
24	4	21	23	4	20	202900.357	-0.010	23.3324	a	90.22
25	1	25	24	1	24	203003.517	0.027	24.9363	a	82.44
30	5	25	30	4	26	203112.867	0.026	16.5933	b	143.72
24	4	20	23	4	19	203179.468	-0.001	23.3326	a	90.25
25	0	25	24	0	24	203273.733	0.019	24.9392	a	82.40
24	3	21	23	3	20	205000.790	0.042	23.6264	a	85.07
24	2	22	23	2	21	206541.142	-0.020	23.8372	a	81.94
21	2	20	20	1	19	207471.062	0.008	9.0389	b	60.85
25	5	20	25	4	21	207737.141	-0.012	13.3359	b	104.09
33	5	29	33	4	30	207894.128	0.048	18.3967	b	170.63
32	5	28	32	4	29	207911.479	0.039	17.7510	b	161.32
34	5	30	34	4	31	207945.427	0.035	19.0420	b	180.23
31	5	27	31	4	28	207985.320	-0.001	17.1064	b	152.29
35	5	31	35	4	32	208078.135	0.013	19.6854	b	190.10
25	2	24	24	2	23	208214.052	-0.009	24.8099	a	86.97
29	5	25	29	4	26	208257.868	-0.005	15.8248	b	135.08
24	5	19	24	4	20	208286.349	-0.001	12.7126	b	97.03
36	5	32	36	4	33	208305.463	0.007	20.3251	b	200.25
26	5	22	26	4	23	208835.101	0.013	13.9326	b	111.38
25	5	21	25	4	22	209041.286	-0.007	13.3116	b	104.04
22	5	17	22	4	18	209131.839	-0.010	11.4872	b	83.76
23	5	19	23	4	20	209440.416	-0.014	12.0853	b	90.22
22	5	18	22	4	19	209625.542	-0.044	11.4796	b	83.74

continued on next page

Table 5 Measured transitions of CH_2DCH_2CN in-plane- continued from previous page

Transition						Obs. Freq.	obs.- calc.	S	Dipole	E_l
J’	K'_a	K'_c	J”	K''_a	K''_c	(MHz)	(MHz)			(cm^{-1})
20	5	15	20	4	16	209717.249	0.009	10.2853	b	71.63
21	5	17	21	4	18	209797.456	-0.023	10.8786	b	77.54
19	5	14	19	4	15	209935.869	0.001	9.6913	b	65.99
26	0	26	25	1	25	210016.606	-0.005	21.8503	b	89.22
19	5	15	19	4	16	210095.346	0.020	9.6893	b	65.98
18	5	13	18	4	14	210115.114	0.026	9.1011	b	60.63
18	5	14	18	4	15	210219.904	0.024	9.0998	b	60.63
27	1	26	26	2	25	210292.455	-0.022	13.9945	b	101.13
16	5	11	16	4	12	210378.953	0.019	7.9283	b	50.77
16	5	12	16	4	13	210420.751	-0.002	7.9279	b	50.77
40	5	36	40	4	37	210429.828	-0.009	22.8052	b	243.67
15	5	10	15	4	11	210473.249	0.004	7.3438	b	46.27
15	5	11	15	4	12	210498.484	0.011	7.3436	b	46.27
25	1	24	24	1	23	210648.123	-0.020	24.8718	a	86.27
25	9	17	24	9	16	210880.985	-0.020	21.7604	a	147.61
25	10	16	24	10	15	210887.671	-0.019	21.0004	a	162.41
25	8	18	24	8	17	210893.254	-0.019	22.4404	a	134.36
25	11	15	24	11	14	210908.154	-0.028	20.1604	a	178.76
25	3	23	24	3	22	210927.693	0.006	24.6312	a	91.50
25	12	14	24	12	13	210939.426	0.002	19.2404	a	196.65
25	13	13	24	13	12	210979.468	-0.032	18.2404	a	216.07
26	1	26	25	1	25	211013.830	0.034	25.9365	a	89.22
25	6	20	24	6	19	211020.394	0.052	23.5603	a	112.53
25	6	19	24	6	18	211020.971	-0.052	23.5603	a	112.53
25	14	12	24	14	11	211027.168	0.012	17.1604	a	237.02
25	15	11	24	15	10	211081.509	-0.032	16.0003	a	259.49
25	16	10	24	16	9	211142.064	0.008	14.7603	a	283.49
25	5	21	24	5	20	211184.622	-0.035	24.0000	a	103.97
25	5	20	24	5	19	211205.283	-0.018	24.0000	a	103.97
25	17	9	24	17	8	211208.264	-0.005	13.4403	a	308.99
26	0	26	25	0	25	211238.030	0.041	25.9387	a	89.18
25	18	8	24	18	7	211279.860	0.001	12.0402	a	336.00
25	19	7	24	19	6	211356.596	0.014	10.5602	a	364.50
25	4	22	24	4	21	211387.864	-0.030	24.3588	a	96.99
25	4	21	24	4	20	211754.476	-0.023	24.3591	a	97.03
27	0	27	26	0	26	219204.852	-0.057	26.9384	a	96.22
26	3	23	25	3	22	222613.281	0.024	25.6590	a	99.04
48	5	44	48	4	45	223018.116	-0.020	26.9241	b	343.77
24	2	23	23	1	22	223615.262	-0.017	11.4810	b	79.51
27	2	26	26	2	25	224490.154	-0.026	26.8155	a	101.13
49	5	45	49	4	46	225548.261	-0.037	27.3242	b	357.52
27	1	26	26	1	25	226570.969	0.095	26.8590	a	100.59
27	3	25	26	3	24	227651.138	-0.050	26.6543	a	105.85
27	11	16	26	11	15	227774.221	-0.083	22.5190	a	193.11
27	8	19	26	8	18	227778.208	-0.060	24.6301	a	148.71
27	7	20	26	7	19	227835.241	-0.087	25.1856	a	137.02
27	7	21	26	7	20	227835.241	-0.046	25.1856	a	137.02
27	13	14	26	13	13	227845.024	0.042	20.7412	a	230.42
27	15	12	26	15	11	227951.108	-0.081	18.6670	a	273.86
27	6	21	26	6	20	227951.108	-0.023	25.6670	a	126.89
27	5	23	26	5	22	228155.714	0.011	26.0740	a	118.34
27	5	22	26	5	21	228196.540	-0.028	26.0740	a	118.35
27	4	23	26	4	22	228967.170	-0.119	26.4062	a	111.44
27	3	24	26	3	23	231429.068	0.022	26.6743	a	106.46
27	2	25	26	2	24	231974.973	-0.012	26.8428	a	103.46
28	1	27	27	1	26	234497.116	-0.059	27.8534	a	108.15
26	2	25	25	1	24	234901.664	-0.011	13.3303	b	93.30
29	1	29	28	1	28	235020.178	0.017	28.9368	a	111.13
29	0	29	28	0	28	235145.122	-0.006	28.9378	a	111.11

continued on next page

Table 5 Measured transitions of CH_2DCH_2CN in-plane- continued from previous page

J'	K'$_a$	K'$_c$	J"	K"$_a$	K"$_c$	Obs. Freq. (MHz)	obs.- calc. (MHz)	S	Dipole	E_l (cm^{-1})
28	9	19	27	9	18	236193.848	-0.048	25.1076	a	169.56
28	11	17	27	11	16	236206.674	-0.110	23.6791	a	200.71
28	12	16	27	12	15	236236.176	0.052	22.8576	a	218.60
28	13	15	27	13	14	236276.598	-0.011	21.9647	a	238.02
28	7	21	27	7	20	236288.325	-0.070	26.2504	a	144.62
28	7	22	27	7	21	236288.325	-0.004	26.2504	a	144.62
28	14	14	27	14	13	236326.451	-0.035	21.0004	a	258.98
28	2	26	27	2	25	240362.646	0.007	27.8417	a	111.20
29	9	20	28	9	19	244631.909	-0.103	26.2074	a	177.44
29	11	18	28	11	17	244638.822	-0.034	24.8281	a	208.59
29	13	16	28	13	15	244707.482	0.027	23.1729	a	245.91
29	5	24	28	5	23	245216.694	-0.042	28.1378	a	133.85
29	2	27	28	2	26	248701.154	-0.076	28.8392	a	119.21
29	3	26	28	3	25	249042.252	-0.028	28.7027	a	122.20
71	3	69	70	2	68	581731.107	0.002	50.9583	b	696.18
69	10	60	68	10	59	581801.782	0.012	67.5542	a	738.00
69	10	59	68	10	58	581806.439	-0.045	67.5542	a	738.00
18	13	6	18	12	7	582029.164	-0.023	5.0897	b	160.34
19	13	7	19	12	8	582064.607	-0.027	5.8179	b	165.68
22	13	10	22	12	11	582177.124	0.106	7.8913	b	183.42
69	9	60	68	9	59	582505.572	0.021	67.8299	a	723.50
59	13	46	59	12	47	582556.178	-0.016	30.0532	b	610.11
57	13	44	57	12	45	582683.177	0.033	28.8600	b	577.22
35	13	22	35	12	23	582685.666	0.032	15.9398	b	289.51
56	13	44	56	12	45	582735.651	0.019	28.2657	b	561.20
37	13	25	37	12	26	582751.975	0.000	17.1194	b	310.05
51	13	39	51	12	40	582900.732	-0.045	25.3134	b	485.28
44	13	32	44	12	33	582912.908	-0.005	21.2162	b	390.79
50	13	38	50	12	39	582916.474	0.016	24.7262	b	470.94
45	13	33	45	12	34	582923.809	0.024	21.8003	b	403.45
49	13	36	49	12	37	582926.975	-0.059	24.1398	b	456.88
68	6	62	67	6	61	583163.419	0.014	67.5275	a	673.26
69	8	61	68	8	60	583883.560	0.048	68.0770	a	710.80
73	1	73	72	1	72	584970.291	-0.010	72.9362	a	707.49
73	0	73	72	0	72	584970.291	-0.016	72.9362	a	707.49
70	5	66	69	5	65	586112.852	0.002	69.5382	a	699.36
17	10	8	16	9	7	587026.949	-0.003	10.2347	b	101.47
17	10	7	16	9	8	587026.949	-0.003	10.2347	b	101.47
69	7	62	68	7	61	587335.352	0.017	68.3032	a	700.29
71	4	68	70	4	67	587989.515	-0.005	70.6170	a	708.11
71	3	68	70	3	67	588216.282	-0.009	70.6183	a	708.06
70	4	66	69	4	65	588230.948	-0.028	69.5588	a	698.83
70	15	56	69	15	55	589198.839	0.026	66.7881	a	854.26
70	16	55	69	16	54	589220.285	-0.011	66.3451	a	878.35
70	14	57	69	14	56	589227.181	-0.010	67.2026	a	831.72
70	17	54	69	17	53	589282.589	0.029	65.8735	a	903.98
70	13	58	69	13	57	589318.443	-0.020	67.5885	a	810.75
70	18	53	69	18	52	589379.100	0.016	65.3734	a	931.13
69	5	64	68	5	63	589476.394	0.012	68.5973	a	686.84
70	12	59	69	12	58	589492.053	0.018	67.9459	a	791.35
70	12	58	69	12	57	589492.053	0.000	67.9459	a	791.35
70	19	52	69	19	51	589505.077	0.009	64.8447	a	959.81
72	3	70	71	3	69	589547.823	-0.018	71.7088	a	715.58
72	2	70	71	2	69	589560.420	-0.008	71.7088	a	715.58
70	20	51	69	20	50	589656.905	0.003	64.2875	a	990.00
70	21	50	69	21	49	589831.784	-0.033	63.7017	a	1021.68
70	22	49	69	22	48	590027.647	-0.007	63.0873	a	1054.86
70	10	61	69	10	60	590225.004	0.031	68.5750	a	757.40
70	10	60	69	10	59	590231.067	0.011	68.5751	a	757.40

continued on next page

Table 5 Measured transitions of CH_2DCH_2CN in-plane- continued from previous page

J'	K'$_a$	K'$_c$	J"	K"$_a$	K"$_c$	Obs. Freq. (MHz)	obs.- calc. (MHz)	S	Dipole	E_l (cm^{-1})
70	23	48	69	23	47	590242.680	-0.023	62.4443	a	1089.51
70	24	47	69	24	46	590475.568	-0.020	61.7728	a	1125.64
70	6	65	69	6	64	590514.222	0.008	69.4441	a	709.16
70	25	46	69	25	45	590725.141	-0.046	61.0727	a	1163.23
70	9	62	69	9	61	590897.085	-0.040	68.8468	a	742.92
70	9	61	69	9	60	590974.749	0.002	68.8469	a	742.93
12	11	2	11	10	1	591017.927	0.015	10.5274	b	96.57
12	11	1	11	10	2	591017.927	0.015	10.5274	b	96.57
23	9	14	22	8	15	591272.704	-0.030	10.5432	b	121.13
70	7	64	69	7	63	592141.887	0.021	69.2948	a	719.08
70	8	62	69	8	61	592473.051	0.026	69.0907	a	730.28
74	1	74	73	1	73	592876.923	-0.008	73.9362	a	727.00
74	0	74	73	0	73	592876.923	-0.013	73.9362	a	727.00
71	5	67	70	5	66	594080.307	-0.004	70.5376	a	718.91
29	8	22	28	7	21	595063.200	0.006	10.9636	b	152.50
18	10	8	17	9	9	595479.907	0.025	10.3954	b	106.25
18	10	9	17	9	8	595479.907	0.025	10.3954	b	106.25
72	4	69	71	4	68	595890.098	0.003	71.6161	a	727.72
71	4	67	70	4	66	595949.234	0.015	70.5547	a	718.45
70	7	63	69	7	62	596200.522	0.040	69.3164	a	719.88
70	5	65	69	5	64	597381.982	0.007	69.5871	a	706.50
73	2	71	72	3	70	597400.251	-0.031	52.9773	b	735.25
73	3	71	72	3	70	597446.669	0.010	72.7084	a	735.25
73	2	71	72	2	70	597456.985	0.000	72.7085	a	735.25
71	15	57	70	15	56	597553.967	0.015	67.8335	a	873.91
71	16	56	70	16	55	597571.045	0.005	67.3967	a	898.00
71	14	58	70	14	57	597588.549	0.016	68.2421	a	851.38
71	17	55	70	17	54	597630.313	0.008	66.9318	a	923.63
71	13	59	70	13	58	597688.446	0.022	68.6226	a	830.41
71	18	54	70	18	53	597724.959	0.018	66.4387	a	950.79
71	19	53	70	19	52	597849.948	0.007	65.9174	a	979.47
71	12	60	70	12	59	597873.990	0.013	68.9750	a	811.02
71	12	59	70	12	58	597873.990	-0.011	68.9750	a	811.02
71	20	52	70	20	51	598001.604	0.063	65.3680	a	1009.66
71	22	50	70	22	49	598373.637	-0.006	64.1847	a	1074.54
71	23	49	70	23	48	598590.108	-0.007	63.5508	a	1109.20
71	10	62	70	10	61	598647.897	0.034	69.5954	a	777.09
71	10	61	70	10	60	598655.695	0.018	69.5954	a	777.09
71	6	66	70	6	65	598671.285	0.026	70.4468	a	728.85
71	24	48	70	24	47	598824.816	-0.027	62.8887	a	1145.34
71	9	63	70	9	62	599350.867	0.009	69.8633	a	762.63
71	9	62	70	9	61	599447.258	-0.054	69.8635	a	762.65
13	11	2	12	10	3	599474.189	0.011	10.5910	b	99.94
13	11	3	12	10	2	599474.189	0.011	10.5910	b	99.94
24	9	16	23	8	15	599705.411	-0.055	10.7335	b	127.61
16	14	3	16	13	4	627769.897	-0.056	2.7574	b	169.90
17	14	4	17	13	5	627806.870	-0.015	3.5832	b	174.68
19	14	6	19	13	7	627885.681	0.005	5.1385	b	185.10
21	14	8	21	13	9	627970.385	-0.060	6.5965	b	196.64
23	14	10	23	13	11	628060.416	-0.003	7.9830	b	209.31
24	14	11	24	13	12	628107.093	-0.003	8.6553	b	216.07
25	14	12	25	13	13	628154.764	0.011	9.3160	b	223.11
26	14	13	26	13	14	628203.262	-0.009	9.9665	b	230.42
74	14	60	74	13	61	628230.589	-0.050	38.6582	b	911.83
27	14	14	27	13	15	628252.556	0.024	10.6081	b	238.02
28	14	15	28	13	16	628302.392	-0.016	11.2419	b	245.91
29	14	16	29	13	17	628352.776	0.005	11.8688	b	254.07
30	14	17	30	13	18	628403.496	0.009	12.4896	b	262.51
32	14	19	32	13	20	628505.411	-0.011	13.7158	b	280.24

continued on next page

Table 5 Measured transitions of CH_2DCH_2CN in-plane- continued from previous page

J'	K'$_a$	K'$_c$	J"	K"$_a$	K"$_c$	Obs. Freq. (MHz)	obs.- calc. (MHz)	S	Dipole	E_l (cm^{-1})
74	5	69	73	5	68	628510.845	0.002	73.5435	a	787.77
33	14	20	33	13	21	628556.355	0.003	14.3223	b	289.53
71	14	57	71	13	58	628585.121	-0.028	36.8196	b	850.34
34	14	21	34	13	22	628607.048	-0.011	14.9252	b	299.10
35	14	22	35	13	23	628657.403	0.017	15.5249	b	308.95
36	14	23	36	13	24	628707.188	0.012	16.1217	b	319.08
37	14	24	37	13	25	628756.266	0.001	16.7161	b	329.49
69	14	55	69	13	56	628776.309	-0.005	35.6034	b	810.75
38	14	25	38	13	26	628804.442	-0.046	17.3083	b	340.18
39	14	26	39	13	27	628851.756	0.083	17.8987	b	351.15
68	14	54	68	13	55	628859.272	-0.001	34.9981	b	791.37
40	14	27	40	13	28	628897.642	-0.003	18.4876	b	362.41
67	14	54	67	13	55	628934.180	-0.037	34.3944	b	772.27
41	14	28	41	13	29	628942.236	0.010	19.0751	b	373.94
42	14	29	42	13	30	628985.211	-0.022	19.6615	b	385.76
77	3	75	76	3	74	629016.274	-0.037	76.7072	a	816.54
65	14	52	65	13	53	629061.114	-0.119	33.1921	b	734.91
44	14	31	44	13	32	629065.787	0.012	20.8320	b	410.23
45	14	32	45	13	33	629102.950	0.025	21.4163	b	422.89
64	14	51	64	13	52	629113.845	-0.034	32.5933	b	716.65
46	14	33	46	13	34	629137.741	0.010	22.0004	b	435.83
47	14	34	47	13	35	629170.018	0.028	22.5842	b	449.05
49	14	36	49	13	37	629226.068	0.026	23.7519	b	476.33
61	14	48	61	13	49	629231.721	0.004	30.8057	b	663.55
50	14	37	50	13	38	629249.428	0.017	24.3360	b	490.39
60	14	47	60	13	48	629258.527	-0.006	30.2126	b	646.40
51	14	38	51	13	39	629269.434	0.049	24.9205	b	504.73
59	14	46	59	13	47	629279.555	-0.003	29.6207	b	629.54
22	10	12	21	9	13	629284.212	-0.049	11.0934	b	128.20
22	10	13	21	9	12	629284.212	-0.049	11.0934	b	128.20
52	14	39	52	13	40	629285.760	0.016	25.5054	b	519.35
58	14	45	58	13	46	629295.074	0.023	29.0299	b	612.96
53	14	40	53	13	41	629298.269	0.008	26.0909	b	534.25
57	14	43	57	13	44	629305.246	-0.018	28.4402	b	596.66
54	14	41	54	13	42	629306.753	0.046	26.6770	b	549.43
78	2	77	77	2	76	630673.652	0.075	77.8158	a	823.08
78	1	77	77	1	76	630673.652	-0.050	77.8158	a	823.08
75	16	60	74	16	59	630945.011	-0.032	71.5894	a	979.40
75	15	61	74	15	60	630947.454	0.007	72.0029	a	955.31
75	17	59	74	17	58	630990.785	0.020	71.1492	a	1005.04
75	14	62	74	14	61	631009.251	0.000	72.3898	a	932.78
75	18	58	74	18	57	631076.581	0.016	70.6824	a	1032.21
75	6	70	74	6	69	631083.508	0.017	74.4536	a	810.36
75	13	63	74	13	62	631146.773	0.007	72.7501	a	911.83
75	13	62	74	13	61	631146.773	0.003	72.7501	a	911.83
75	19	57	74	19	56	631196.557	0.013	70.1889	a	1060.91
75	20	56	74	20	55	631346.294	0.014	69.6687	a	1091.12
75	12	64	74	12	63	631384.587	0.043	73.0838	a	892.47
75	12	63	74	12	62	631384.587	-0.038	73.0838	a	892.47
75	21	55	74	21	54	631522.405	0.011	69.1219	a	1122.84
75	22	54	74	22	53	631722.282	0.027	68.5485	a	1156.05
74	7	67	73	7	66	631755.465	-0.011	73.3729	a	801.21
75	11	65	74	11	64	631761.127	-0.022	73.3909	a	874.73
75	11	64	74	11	63	631762.599	0.012	73.3909	a	874.73
75	23	53	74	23	52	631943.783	-0.002	67.9483	a	1190.74
75	24	52	74	24	51	632185.333	0.017	67.3216	a	1226.91
75	10	66	74	10	65	632336.096	0.013	73.6714	a	858.65
75	10	65	74	10	64	632356.452	0.000	73.6714	a	858.66
79	1	79	78	1	78	632371.594	0.012	78.9363	a	828.52

continued on next page

Table 5 Measured transitions of CH_2DCH_2CN in-plane- continued from previous page

J'	K'$_a$	K'$_c$	J"	K"$_a$	K"$_c$	Obs. Freq. (MHz)	obs.- calc. (MHz)	S	Dipole	E_l (cm^{-1})
79	0	79	78	0	78	632371.594	0.010	78.9363	a	828.52
75	25	51	74	25	50	632445.528	0.037	66.6681	a	1264.54
75	26	50	74	26	49	632723.192	-0.001	65.9880	a	1303.63
75	27	49	74	27	48	633017.521	0.033	65.2812	a	1344.16
75	9	67	74	9	66	633161.457	-0.009	73.9251	a	844.29
17	11	7	16	10	6	633306.794	0.031	11.0454	b	116.27
17	11	6	16	10	7	633306.794	0.031	11.0454	b	116.27
75	28	48	74	28	47	633327.518	-0.068	64.5478	a	1386.13
75	9	66	74	9	65	633381.795	-0.007	73.9256	a	844.32
28	9	20	27	8	19	633395.890	-0.109	11.5006	b	156.31
76	5	72	75	5	71	633745.475	0.015	75.5329	a	820.64
75	7	69	74	7	68	633834.261	-0.007	74.3321	a	820.63
74	6	68	73	6	67	634415.440	-0.029	73.5674	a	794.29
77	4	74	76	4	73	635336.223	0.004	76.6122	a	829.74
77	3	74	76	3	73	635415.536	0.018	76.6127	a	829.73
75	8	67	74	8	66	635686.875	-0.024	74.1549	a	831.97
75	5	70	74	5	69	636199.175	-0.017	74.5330	a	808.74
78	3	76	77	3	75	636902.223	-0.001	77.7069	a	837.53
79	2	78	78	2	77	638563.032	0.064	78.8158	a	844.11
79	1	78	78	1	77	638563.032	-0.036	78.8158	a	844.11
76	16	61	75	16	60	639281.092	-0.010	72.6344	a	1000.45
76	15	62	75	15	61	639288.856	-0.011	73.0425	a	976.36
76	17	60	75	17	59	639323.053	0.010	72.2000	a	1026.09
76	14	63	75	14	62	639358.079	-0.018	73.4243	a	953.83
76	18	59	75	18	58	639406.320	0.014	71.7393	a	1053.26
76	13	64	75	13	63	639505.830	-0.003	73.7799	a	932.88
76	13	63	75	13	62	639505.830	-0.008	73.7799	a	932.88
76	19	58	75	19	57	639524.752	-0.002	71.2523	a	1081.97
76	20	57	75	20	56	639673.757	-0.031	70.7390	a	1112.18
76	12	65	75	12	64	639757.808	0.017	74.1092	a	913.53
76	12	64	75	12	63	639757.808	-0.091	74.1092	a	913.53
76	21	56	75	21	55	639849.889	-0.007	70.1994	a	1143.90
76	22	55	75	22	54	640050.348	0.002	69.6334	a	1177.12
76	11	66	75	11	65	640154.402	-0.001	74.4123	a	895.80
76	11	65	75	11	64	640156.256	-0.010	74.4123	a	895.80
80	1	80	79	1	79	640262.605	0.010	79.9363	a	849.61
80	0	80	79	0	79	640262.605	0.009	79.9363	a	849.61
76	23	54	75	23	53	640272.990	0.011	69.0412	a	1211.82
75	7	68	74	7	67	640636.381	-0.049	74.3877	a	822.28
76	25	52	75	25	51	640778.188	-0.012	67.7778	a	1285.64
76	10	66	75	10	65	640782.792	-0.021	74.6892	a	879.75
76	9	68	75	9	67	641611.682	-0.025	74.9396	a	865.41
77	5	73	76	5	72	641649.704	0.005	76.5318	a	841.78
29	9	21	28	8	20	641806.039	-0.080	11.6925	b	164.19
29	9	20	28	8	21	641806.039	-0.083	11.6925	b	164.19
76	7	70	75	7	69	642114.324	-0.009	75.3380	a	841.77
76	8	69	75	8	68	642454.900	-0.035	75.1607	a	852.83
77	4	73	76	4	72	642463.583	-0.024	76.5376	a	841.60

Table 6. Measured transitions of the ground vibrational state of CH_2DCH_2CN out-of-plane

J'	K'$_a$	K'$_c$	J"	K"$_a$	K"$_c$	Obs. Freq. (MHz)	obs.- calc. (MHz)	S	Dipole	E$_l$ (cm^{-1})
22	4	18	21	5	17	8505.160	-0.007	3.3575	b	84.32
6	2	4	7	1	7	8520.324	0.006	0.8664	b	8.58
1	0	1	0	0	0	8693.720	0.004	1.0000	a	0.00
29	4	25	29	4	26	8713.615	0.001	0.9523	a	137.58
10	1	10	9	2	7	8777.717	-0.014	1.1077	b	15.88
38	5	33	38	5	34	8862.059	0.000	1.1166	a	232.89
38	9	30	39	8	31	9150.310	0.088	5.8015	b	270.62
10	3	7	11	2	10	9258.390	-0.006	1.5568	b	21.87
6	1	5	6	1	6	9927.536	0.018	0.3104	a	6.61
13	2	11	13	2	12	9979.460	0.036	0.5423	a	29.09
21	3	18	21	3	19	9984.452	0.021	0.7427	a	73.33
19	5	15	20	4	16	9985.854	-0.039	2.9272	b	72.07
27	5	23	26	6	20	10265.926	0.001	4.1274	b	126.75
19	5	14	20	4	17	10539.037	-0.016	2.9244	b	72.05
27	5	22	26	6	21	10644.847	-0.027	4.1292	b	126.75
30	4	26	30	4	27	11042.694	-0.011	0.9021	a	146.32
39	5	34	39	5	35	11094.789	-0.011	1.0672	a	244.26
33	8	26	34	7	27	11610.053	0.074	5.0293	b	206.59
33	8	25	34	7	28	11621.005	0.054	5.0292	b	206.59
14	4	11	15	3	12	12058.793	-0.032	2.1552	b	41.11
18	3	16	17	4	13	12382.174	-0.003	2.7638	b	55.48
22	3	19	22	3	20	12721.742	-0.002	0.6935	a	79.72
32	6	27	31	7	24	12898.634	-0.053	4.9010	b	177.81
14	2	12	14	2	13	12930.827	0.052	0.4944	a	33.13
32	6	26	31	7	25	13016.012	-0.051	4.9014	b	177.81
7	1	6	7	1	7	13227.117	0.027	0.2693	a	8.58
11	1	11	10	2	8	13439.551	-0.039	1.1165	b	18.82
9	3	7	10	2	8	13519.020	-0.045	1.3915	b	18.82
14	4	10	15	3	13	13640.468	-0.025	2.1449	b	41.06
40	5	35	40	5	36	13754.633	-0.010	1.0186	a	255.93
31	4	27	31	4	28	13820.718	-0.018	0.8536	a	155.35
28	7	22	29	6	23	14115.276	-0.014	4.2564	b	151.18
28	7	21	29	6	24	14152.262	-0.007	4.2563	b	151.18
14	2	13	13	3	10	14172.439	0.002	2.0809	b	32.66
4	2	3	5	1	4	15060.282	0.002	0.6499	b	5.16
5	2	3	6	1	6	15209.902	0.020	0.7182	b	6.61
4	0	4	3	1	3	15400.948	0.029	1.6290	b	2.38
8	1	7	7	2	6	15742.581	0.064	1.5361	b	10.87
23	3	20	23	3	21	15947.741	0.000	0.6477	a	86.39
23	4	20	22	5	17	16299.113	0.032	3.5581	b	90.72
15	2	13	15	2	14	16371.830	0.052	0.4527	a	37.45
23	6	18	24	5	19	16632.881	-0.048	3.4829	b	104.40
23	6	17	24	5	20	16752.974	-0.045	3.4825	b	104.39
18	3	15	17	4	14	16865.617	0.051	2.8063	b	55.47
2	1	2	1	1	1	16914.335	0.001	1.5000	a	0.97
8	1	7	8	1	8	16988.077	0.043	0.2383	a	10.83
13	2	11	12	3	10	16998.902	0.054	2.0936	b	28.86
2	0	2	1	0	1	17379.240	0.004	1.9998	a	0.29
1	1	0	1	0	1	20912.340	0.022	1.5000	b	0.29
2	1	1	2	0	2	21393.790	0.010	2.4712	b	0.87
3	1	2	3	0	3	22131.110	0.015	3.3993	b	1.74
3	1	3	2	1	2	25366.350	0.025	2.6666	a	1.54
3	0	3	2	0	2	26048.440	0.055	2.9992	a	0.87
3	2	2	2	2	1	26081.880	0.075	1.6667	a	3.63
3	2	1	2	2	0	26114.200	-0.066	1.6667	a	3.63
3	1	2	2	1	1	26785.620	-0.081	2.6666	a	1.58
1	1	1	0	0	0	29132.850	0.016	1.0000	b	0.00
2	1	2	1	0	1	37353.490	0.038	1.5000	b	0.29

continued on next page

Table 6 Measured transitions of CH_2DCH_2CN out-of-plane- continued from previous page

Transition						Obs. Freq.	obs.- calc.	S	Dipole	E_l
J'	K'$_a$	K'$_c$	J"	K"$_a$	K"$_c$	(MHz)	(MHz)			(cm^{-1})
17	1	17	16	1	16	142528.858	0.049	16.9243	a	38.88
18	0	18	17	1	17	148133.398	0.023	14.1279	b	43.64
17	1	16	16	1	15	149632.173	0.100	16.8969	a	40.95
18	1	18	17	1	17	150801.915	0.067	17.9257	a	43.64
28	4	25	28	3	26	151323.292	-0.020	15.4325	b	124.08
18	0	18	17	0	17	151404.189	0.023	17.9365	a	43.53
48	4	44	48	3	45	154670.839	0.007	29.8448	b	351.99
55	6	49	55	5	50	155483.536	0.012	41.9160	b	469.31
19	2	18	18	2	17	163656.895	0.006	18.7673	a	52.13
19	9	10	18	9	9	165358.924	0.088	14.7373	a	105.41
19	11	8	18	11	7	165380.203	0.022	12.6320	a	132.90
19	7	13	18	7	12	165387.922	0.035	16.4215	a	83.39
19	7	12	18	7	11	165387.922	0.033	16.4215	a	83.39
19	12	7	18	12	6	165402.146	0.013	11.4214	a	148.69
19	13	6	18	13	5	165429.794	0.013	10.1056	a	165.83
19	6	14	18	6	13	165440.110	0.079	17.1057	a	74.45
19	6	13	18	6	12	165440.110	-0.035	17.1057	a	74.45
19	5	15	18	5	14	165543.320	0.039	17.6845	a	66.88
19	5	14	18	5	13	165548.205	0.003	17.6845	a	66.88
19	3	17	18	3	16	165566.094	0.024	18.5216	a	55.89
19	4	16	18	4	15	165708.588	0.052	18.1575	a	60.71
19	4	15	18	4	14	165833.385	0.010	18.1575	a	60.71
19	1	18	18	1	17	166510.726	0.044	18.8835	a	51.22
19	3	16	18	3	15	167067.988	0.004	18.5252	a	56.03
20	1	20	19	1	19	167319.526	0.030	19.9274	a	53.97
20	0	20	19	0	19	167738.256	0.052	19.9335	a	53.90
19	2	17	18	2	16	169057.543	0.064	18.7987	a	53.12
20	9	12	19	9	11	174065.366	0.033	15.9505	a	110.93
20	10	11	19	10	10	174069.457	0.020	15.0005	a	123.99
20	8	13	19	8	12	174074.868	0.020	16.8005	a	99.23
20	11	10	19	11	9	174083.423	-0.023	13.9505	a	138.42
20	13	8	19	13	7	174133.208	0.044	11.5504	a	171.35
20	14	6	19	14	5	174166.584	0.007	10.2003	a	189.85
20	6	14	19	6	13	174167.838	-0.058	18.2004	a	79.97
20	15	6	19	15	5	174204.765	-0.006	8.7503	a	209.70
20	3	18	19	3	17	174251.050	0.049	19.5440	a	61.41
20	5	16	19	5	15	174289.302	0.011	18.7502	a	72.40
20	5	15	19	5	14	174297.109	-0.009	18.7502	a	72.41
16	2	15	15	1	14	174413.863	0.022	6.3153	b	36.25
20	4	16	19	4	15	174648.267	0.088	19.1995	a	66.25
20	1	19	19	1	18	174861.548	0.048	19.8754	a	56.77
21	1	21	20	1	20	175566.082	0.057	20.9280	a	59.55
21	0	21	20	0	20	175910.461	0.010	20.9326	a	59.50
20	3	17	19	3	16	176120.441	0.020	19.5497	a	61.61
21	1	21	20	0	20	177311.132	0.020	17.2755	b	59.50
20	2	18	19	2	17	177965.421	0.021	19.8080	a	58.76
27	5	22	27	4	23	178625.854	-0.024	14.9558	b	121.15
38	4	35	38	3	36	178861.263	0.026	19.0072	b	220.65
22	0	22	21	1	21	182686.166	0.024	18.2760	b	65.41
21	9	13	20	9	12	182772.373	0.037	17.1434	a	116.73
21	10	12	20	10	11	182773.915	0.035	16.2386	a	129.79
21	12	10	20	12	9	182807.831	0.033	14.1433	a	160.01
21	7	14	20	7	13	182823.264	-0.007	18.6672	a	94.72
21	7	15	20	7	14	182823.264	0.000	18.6672	a	94.72
23	1	22	22	2	21	182832.163	-0.003	11.3730	b	75.66
21	14	8	20	14	7	182870.150	0.011	11.6670	a	195.66
21	15	7	20	15	6	182909.520	0.048	10.2860	a	215.51
21	3	19	20	3	18	182921.801	0.019	20.5639	a	67.22
21	16	6	20	16	5	182953.500	-0.006	8.8098	a	236.71

continued on next page

Table 6 Measured transitions of CH_2DCH_2CN out-of-plane- continued from previous page

Transition						Obs. Freq.	obs.- calc.	S	Dipole	E_l
J’	K’$_a$	K’$_c$	J”	K”$_a$	K”$_c$	(MHz)	(MHz)			(cm^{-1})
21	5	17	20	5	16	183040.065	0.024	19.8097	a	78.22
21	5	16	20	5	15	183052.204	0.015	19.8097	a	78.22
21	1	20	20	1	19	183156.491	0.028	20.8668	a	62.60
21	4	18	20	4	17	183235.279	0.045	20.2373	a	72.05
29	5	25	29	4	26	183324.143	0.007	16.1220	b	137.58
22	5	17	22	4	18	183340.741	0.024	11.6690	b	84.61
30	5	26	30	4	27	183349.101	0.013	16.7711	b	146.32
28	5	24	28	4	25	183371.270	0.029	15.4730	b	129.13
27	5	23	27	4	24	183475.472	0.042	14.8256	b	120.98
21	4	17	20	4	16	183482.250	0.051	20.2374	a	72.07
26	5	22	26	4	23	183622.883	0.017	14.1812	b	113.11
47	6	41	47	5	42	183663.482	-0.046	30.1738	b	347.25
32	5	28	32	4	29	183679.458	0.019	18.0612	b	164.66
25	5	21	25	4	22	183801.037	0.018	13.5407	b	105.54
22	1	22	21	1	21	183805.585	0.016	21.9283	a	65.41
24	5	20	24	4	21	183998.807	0.021	12.9050	b	98.26
33	5	29	33	4	30	184018.409	0.013	18.6975	b	174.27
38	2	36	38	1	37	184050.879	-0.018	13.3909	b	214.15
22	0	22	21	0	21	184086.807	0.004	21.9318	a	65.36
23	5	19	23	4	20	184206.554	-0.004	12.2744	b	91.27
20	5	15	20	4	16	184294.894	0.003	10.4236	b	72.07
22	5	18	22	4	19	184416.268	0.018	11.6493	b	84.57
34	5	30	34	4	31	184495.975	0.021	19.3245	b	184.17
21	5	17	21	4	18	184621.271	-0.001	11.0296	b	78.17
19	5	14	19	4	15	184645.975	0.023	9.8112	b	66.25
20	5	16	20	4	17	184816.474	0.010	10.4153	b	72.05
33	1	32	33	0	33	184881.305	0.072	6.6444	b	157.08
18	5	13	18	4	14	184931.148	0.024	9.2043	b	60.71
19	5	15	19	4	16	184997.996	-0.003	9.8059	b	66.23
35	5	31	35	4	32	185128.989	-0.016	19.9392	b	194.35
17	5	12	17	4	13	185161.534	0.028	8.6021	b	55.48
18	5	14	18	4	15	185163.272	0.018	9.2011	b	60.71
21	3	18	20	3	17	185204.626	0.027	20.5725	a	67.48
22	1	22	21	0	21	185206.240	0.010	18.2990	b	65.36
17	5	13	17	4	14	185310.689	0.024	8.6001	b	55.47
16	5	12	16	4	13	185439.572	-0.006	8.0022	b	50.53
15	5	10	15	4	11	185493.786	0.005	7.4069	b	45.88
18	2	17	17	1	16	185558.635	0.006	7.5953	b	45.94
14	5	9	14	4	10	185610.074	0.017	6.8115	b	41.52
14	5	10	14	4	11	185642.960	0.090	6.8112	b	41.52
13	5	9	13	4	10	185719.028	-0.050	6.2153	b	37.45
12	5	8	12	4	9	185780.191	0.023	5.6166	b	33.67
36	5	32	36	4	33	185933.927	-0.013	20.5386	b	204.82
22	1	21	21	1	20	191400.724	0.056	21.8580	a	68.71
23	1	23	22	1	22	192038.951	-0.004	22.9286	a	71.54
23	0	23	22	0	22	192267.161	0.043	22.9312	a	71.50
23	2	22	22	2	21	197330.242	0.023	22.7894	a	75.66
23	1	22	22	1	21	199601.120	0.024	22.8495	a	75.10
44	5	40	44	4	41	200150.336	-0.037	24.4636	b	298.80
23	10	14	22	10	13	200183.163	0.011	18.6528	a	142.28
23	9	15	22	9	14	200187.961	0.009	19.4789	a	129.22
23	11	13	22	11	12	200192.255	0.003	17.7397	a	156.71
23	3	21	22	3	20	200213.919	0.030	22.5973	a	79.72
23	13	11	22	13	10	200239.957	-0.016	15.6527	a	189.65
23	14	10	22	14	9	200275.102	-0.013	14.4787	a	208.15
23	15	9	22	15	8	200316.428	0.042	13.2178	a	228.01
23	16	8	22	16	7	200363.098	-0.032	11.8699	a	249.21
23	6	18	22	6	17	200369.921	-0.004	21.4353	a	98.27
23	6	17	22	6	16	200370.868	-0.019	21.4353	a	98.27

continued on next page

Table 6 Measured transitions of CH_2DCH_2CN out-of-plane- continued from previous page

Transition						Obs. Freq.	obs.- calc.	S	Dipole	E_l
J'	K'$_a$	K'$_c$	J"	K"$_a$	K"$_c$	(MHz)	(MHz)			(cm^{-1})
23	17	7	22	17	6	200414.871	-0.006	10.4351	a	271.75
24	0	24	23	0	23	200450.999	-0.003	23.9308	a	77.92
23	5	19	22	5	18	200555.950	0.017	21.9132	a	90.72
23	5	18	22	5	17	200583.328	-0.028	21.9132	a	90.72
23	4	20	22	4	19	200765.597	-0.028	22.3029	a	84.57
28	2	26	27	3	25	201109.133	-0.022	8.6888	b	115.98
24	1	24	23	0	23	201158.187	-0.009	20.3402	b	77.92
23	4	19	22	4	18	201219.120	-0.005	22.3033	a	84.61
42	6	36	42	5	37	202607.143	0.029	24.9603	b	280.81
45	5	41	45	4	42	203030.308	-0.047	24.8177	b	311.82
23	3	20	22	3	19	203439.898	0.011	22.6142	a	80.14
25	1	24	24	2	23	203474.049	0.015	13.4743	b	89.10
23	2	21	22	2	20	204412.807	0.013	22.8227	a	77.46
24	1	23	23	1	22	207765.974	-0.042	23.8417	a	81.76
25	0	25	24	1	24	207930.743	0.006	21.3481	b	84.63
22	2	21	21	1	20	208169.578	-0.020	10.8238	b	68.71
40	6	34	40	5	35	208426.395	0.011	23.2737	b	256.39
25	0	25	24	0	24	208637.929	-0.003	24.9304	a	84.60
24	3	22	23	3	21	208832.076	0.004	23.6112	a	86.39
24	10	15	23	10	14	208887.975	-0.010	19.8340	a	148.96
24	11	14	23	11	13	208894.805	-0.016	18.9590	a	163.39
24	9	16	23	9	15	208896.597	-0.011	20.6257	a	135.89
24	12	13	23	12	12	208913.294	-0.006	18.0006	a	179.18
24	8	17	23	8	16	208927.129	0.004	21.3340	a	124.20
24	13	12	23	13	11	208941.021	-0.012	16.9589	a	196.33
24	14	11	23	14	10	208976.443	-0.016	15.8339	a	214.83
24	7	17	23	7	16	208991.148	-0.025	21.9589	a	113.89
24	7	18	23	7	17	208991.148	0.013	21.9589	a	113.89
24	15	10	23	15	9	209018.496	-0.023	14.6255	a	234.69
24	16	9	23	16	8	209066.456	-0.015	13.3338	a	255.89
24	6	19	23	6	18	209110.898	-0.009	22.5005	a	104.95
24	6	18	23	6	17	209112.431	-0.018	22.5005	a	104.95
24	5	20	23	5	19	209320.973	-0.013	22.9584	a	97.41
24	5	19	23	5	18	209361.034	0.018	22.9584	a	97.41
24	4	21	23	4	20	209528.750	-0.009	23.3315	a	91.27
24	4	20	23	4	19	210128.077	0.024	23.3321	a	91.32
39	6	33	39	5	34	210903.066	-0.004	22.4826	b	244.63
25	1	24	24	1	23	215904.186	-0.037	24.8346	a	88.69
26	1	26	25	1	25	216709.260	0.030	25.9290	a	91.58
26	0	26	25	0	25	216827.371	0.029	25.9301	a	91.56
39	6	34	39	5	35	220895.121	0.027	22.1752	b	244.26
44	6	39	44	5	40	221000.246	0.022	25.5516	b	305.48
45	6	40	45	5	41	221403.570	0.022	26.2021	b	318.59
37	6	32	37	5	33	221442.641	-0.036	20.8092	b	221.81
32	6	26	32	5	27	221580.826	0.008	17.4900	b	170.85
25	3	22	24	3	21	221701.029	0.013	24.6520	a	94.02
25	2	23	24	2	22	221775.867	-0.028	24.8219	a	91.38
36	6	31	36	5	32	221783.590	0.004	20.1298	b	211.02
49	3	46	49	2	47	221905.532	0.019	20.2896	b	358.79
46	6	41	46	5	42	221972.767	-0.026	26.8382	b	331.99
26	2	25	25	2	24	222378.448	0.002	25.7972	a	96.24
30	6	24	30	5	25	223124.915	0.049	16.1720	b	152.47
27	1	26	26	2	25	223206.302	-0.030	15.6299	b	103.66
32	6	27	32	5	28	223325.004	0.036	17.4578	b	170.79
48	6	43	48	5	44	223670.889	0.008	28.0555	b	359.64
31	6	26	31	5	27	223710.153	-0.049	16.8040	b	161.47
29	6	23	29	5	24	223740.591	0.028	15.5256	b	143.72
43	3	41	43	2	42	223877.433	-0.001	13.3561	b	271.88
26	1	25	25	1	24	224024.233	-0.021	25.8285	a	95.89

continued on next page

Table 6 Measured transitions of CH_2DCH_2CN out-of-plane- continued from previous page

Transition						Obs. Freq.	obs.- calc.	S	Dipole	E_l
J'	K'$_a$	K'$_c$	J"	K"$_a$	K"$_c$	(MHz)	(MHz)			(cm^{-1})
30	6	25	30	5	26	224082.227	-0.002	16.1563	b	152.43
28	6	22	28	5	23	224270.732	-0.038	14.8866	b	135.27
29	6	24	29	5	25	224436.659	0.008	15.5147	b	143.70
27	0	27	26	1	26	224577.317	-0.043	23.3825	b	98.81
27	6	21	27	5	22	224727.225	0.005	14.2545	b	127.11
28	6	23	28	5	24	224770.104	-0.072	14.8792	b	135.25
27	1	27	26	1	26	224924.597	-0.033	26.9290	a	98.81
15	3	13	14	2	12	224937.468	0.027	4.5991	b	33.56
27	0	27	26	0	26	225018.660	-0.014	26.9298	a	98.80
27	6	22	27	5	23	225080.515	0.013	14.2495	b	127.10
26	6	20	26	5	21	225120.022	0.029	13.6288	b	119.24
25	6	19	25	5	20	225457.701	-0.010	13.0089	b	111.67
25	6	20	25	5	21	225626.594	0.015	13.0068	b	111.67
24	6	18	24	5	19	225747.708	-0.013	12.3943	b	104.40
24	6	19	24	5	20	225861.555	-0.028	12.3929	b	104.39
23	6	17	23	5	18	225996.301	0.014	11.7845	b	97.41
26	3	24	25	3	23	226006.141	-0.005	25.6344	a	100.61
23	6	18	23	5	19	226071.609	-0.053	11.7836	b	97.41
26	10	16	25	10	15	226298.040	-0.017	22.1546	a	163.18
26	11	15	25	11	14	226299.334	-0.010	21.3469	a	177.61
26	9	17	25	9	16	226315.629	-0.091	22.8853	a	150.12
26	13	13	25	13	12	226341.161	-0.003	19.5006	a	210.56
26	8	19	25	8	18	226360.507	-0.032	23.5392	a	138.43
26	8	18	25	8	17	226360.507	-0.034	23.5392	a	138.43
26	14	12	25	14	11	226376.644	-0.038	18.4621	a	229.07
26	15	11	25	15	10	226419.853	-0.084	17.3467	a	248.92
26	7	20	25	7	19	226447.359	0.030	24.1160	a	128.12
26	7	19	25	7	18	226447.359	-0.081	24.1160	a	128.12
26	6	21	25	6	20	226604.034	-0.017	24.6159	a	119.19
26	6	20	25	6	19	226607.781	0.010	24.6159	a	119.19
26	5	22	25	5	21	226864.385	-0.046	25.0384	a	111.67
26	5	21	25	5	20	226945.488	0.000	25.0384	a	111.67
26	4	23	25	4	22	227042.567	-0.018	25.3816	a	105.54
26	2	24	25	2	23	230366.499	-0.024	25.8185	a	98.78
26	3	23	25	3	22	230815.001	0.015	25.6693	a	101.41
28	1	28	27	1	27	233136.779	-0.007	27.9290	a	106.31
28	0	28	27	0	27	233211.372	-0.036	27.9296	a	106.30
27	11	17	26	11	16	235001.250	-0.024	22.5193	a	185.16
27	10	18	26	10	17	235003.275	-0.025	23.2971	a	170.73
27	12	16	26	12	15	235014.661	-0.037	21.6674	a	200.95
27	9	19	26	9	18	235026.176	-0.043	24.0008	a	157.67
27	13	15	26	13	14	235040.114	-0.062	20.7414	a	218.11
27	8	20	26	8	19	235079.233	-0.004	24.6304	a	145.98
27	8	19	26	8	18	235079.233	-0.008	24.6304	a	145.98
28	2	27	27	2	26	238991.357	-0.076	27.7998	a	111.35
28	1	27	27	1	26	240238.941	-0.040	27.8191	a	111.10
28	11	17	27	11	16	243702.950	-0.016	23.6794	a	193.00
28	8	21	27	8	20	243799.325	-0.006	25.7151	a	153.82
28	8	20	27	8	19	243799.325	-0.013	25.7151	a	153.82
28	7	22	27	7	21	243913.271	0.114	26.2507	a	143.52
28	6	23	27	6	22	244112.916	0.055	26.7148	a	134.60
28	6	22	27	6	21	244121.183	-0.037	26.7148	a	134.60
28	5	24	27	5	23	244423.079	-0.109	27.1069	a	127.10
28	4	25	27	4	24	244527.299	-0.077	27.4238	a	120.98
28	5	23	27	5	22	244577.683	0.014	27.1070	a	127.11
28	4	24	27	4	23	246096.865	-0.093	27.4278	a	121.15
28	2	26	27	2	25	247353.324	0.026	27.8062	a	114.43
28	3	25	27	3	24	248960.772	-0.075	27.6995	a	117.11
67	18	50	66	18	49	581757.146	-0.007	62.1673	a	863.83

continued on next page

Table 6 Measured transitions of CH_2DCH_2CN out-of-plane- continued from previous page

J'	K'$_a$	K'$_c$	J"	K"$_a$	K"$_c$	Obs. Freq. (MHz)	obs.- calc. (MHz)	S	Dipole	E_l (cm^{-1})
67	15	53	66	15	52	581767.715	0.021	63.6454	a	796.00
67	19	49	66	19	48	581826.168	0.000	61.6149	a	889.16
67	14	54	66	14	53	581872.074	-0.020	64.0785	a	776.14
67	20	48	66	20	47	581922.602	-0.002	61.0326	a	915.83
67	6	62	66	6	61	582016.681	-0.029	66.3847	a	668.29
67	21	47	66	21	46	582043.028	-0.008	60.4206	a	943.83
67	13	55	66	13	54	582050.638	-0.002	64.4818	a	757.67
67	13	54	66	13	53	582050.638	-0.006	64.4818	a	757.67
67	22	46	66	22	45	582184.782	-0.020	59.7786	a	973.17
67	12	56	66	12	55	582328.371	0.012	64.8552	a	740.61
67	12	55	66	12	54	582328.371	-0.080	64.8552	a	740.61
70	2	69	69	2	68	582330.386	-0.033	69.7924	a	681.64
67	23	45	66	23	44	582345.796	-0.006	59.1069	a	1003.82
67	24	44	66	24	43	582524.381	0.026	58.4053	a	1035.79
66	7	59	65	7	58	582691.375	0.028	65.2984	a	659.47
67	25	43	66	25	42	582719.132	0.035	57.6738	a	1069.06
67	11	57	66	11	56	582744.491	-0.100	65.1989	a	724.99
67	11	56	66	11	55	582746.208	0.009	65.1989	a	724.99
67	26	42	66	26	41	582928.887	-0.019	56.9125	a	1103.64
67	27	41	66	27	40	583152.842	-0.008	56.1214	a	1139.50
67	10	58	66	10	57	583359.724	0.037	65.5129	a	710.83
67	10	57	66	10	56	583382.246	-0.001	65.5129	a	710.84
67	28	40	66	28	39	583390.131	-0.014	55.3004	a	1176.65
67	29	39	66	29	38	583640.125	0.002	54.4495	a	1215.07
67	30	38	66	30	37	583902.206	-0.006	53.5688	a	1254.76
67	31	37	66	31	36	584175.914	0.002	52.6583	a	1295.71
67	9	59	66	9	58	584222.814	0.012	65.7968	a	698.20
67	9	58	66	9	57	584463.798	0.045	65.7973	a	698.23
67	7	61	66	7	60	584856.446	-0.034	66.2505	a	677.37
68	5	64	67	5	63	584859.516	-0.009	67.4728	a	678.14
67	8	60	66	8	59	585097.698	-0.019	66.0478	a	687.10
66	6	60	65	6	59	585163.024	-0.003	65.5123	a	653.40
27	9	19	26	8	18	585418.161	-0.085	11.2126	b	145.98
27	9	18	26	8	19	585418.161	-0.090	11.2126	b	145.98
68	4	64	67	4	63	585716.582	-0.034	67.4796	a	677.96
69	4	66	68	4	65	586689.334	0.006	68.5624	a	686.91
69	3	66	68	3	65	586758.159	0.005	68.5628	a	686.90
67	8	59	66	8	58	586882.878	0.037	66.0541	a	687.37
67	5	62	66	5	61	586929.418	-0.063	66.4674	a	666.93
70	3	68	69	3	67	588517.311	-0.008	69.6695	a	694.52
70	2	68	69	2	67	588520.464	-0.003	69.6695	a	694.52
18	11	8	17	10	7	589181.422	-0.012	11.1686	b	113.25
18	11	7	17	10	8	589181.422	-0.012	11.1686	b	113.25
68	6	63	67	6	62	590302.417	-0.015	67.3854	a	687.70
68	17	52	67	17	51	590329.076	0.012	63.7534	a	859.26
68	16	53	67	16	52	590334.835	0.005	64.2389	a	836.65
68	18	51	67	18	50	590362.588	0.003	63.2385	a	883.24
68	15	54	67	15	53	590388.453	0.006	64.6950	a	815.41
68	19	50	67	19	49	590429.134	0.005	62.6942	a	908.57
71	2	70	70	2	69	590443.311	-0.027	70.7924	a	701.07
71	1	70	70	1	69	590443.311	-0.107	70.7924	a	701.07
68	14	55	67	14	54	590501.948	0.009	65.1217	a	795.55
68	20	49	67	20	48	590524.012	0.005	62.1205	a	935.24
68	21	48	67	21	47	590643.635	-0.008	61.5174	a	963.25
68	13	56	67	13	55	590692.780	0.023	65.5190	a	777.09
68	22	47	67	22	46	590785.258	-0.001	60.8850	a	992.59
68	23	46	67	23	45	590946.692	0.029	60.2231	a	1023.25
68	12	57	67	12	56	590987.344	0.070	65.8871	a	760.04
68	12	56	67	12	55	590987.344	-0.056	65.8871	a	760.04

continued on next page

Table 6 Measured transitions of CH_2DCH_2CN out-of-plane- continued from previous page

J’	K’$_a$	K’$_c$	J”	K”$_a$	K”$_c$	Obs. Freq. (MHz)	obs.- calc. (MHz)	S	Dipole	E_l (cm^{-1})
68	24	45	67	24	44	591126.115	0.013	59.5318	a	1055.22
68	25	44	67	25	43	591322.161	0.006	58.8111	a	1088.50
68	11	58	67	11	57	591426.980	-0.003	66.2258	a	744.43
68	11	57	67	11	56	591429.136	0.001	66.2258	a	744.43
68	26	43	67	26	42	591533.674	0.019	58.0610	a	1123.08
68	27	42	67	27	41	591759.640	0.011	57.2814	a	1158.95
23	10	13	22	9	14	591794.399	-0.085	11.2235	b	129.22
67	7	60	66	7	59	591918.946	0.040	66.3172	a	678.91
68	28	41	67	28	40	591999.278	0.015	56.4725	a	1196.11
68	10	59	67	10	58	592074.466	0.021	66.5351	a	730.29
68	10	58	67	10	57	592103.637	0.009	66.5352	a	730.30
68	9	60	67	9	59	592970.239	0.014	66.8149	a	717.68
69	5	65	68	5	64	592985.326	0.029	68.4713	a	697.65
68	9	59	67	9	58	593270.447	0.036	66.8155	a	717.72
68	7	62	67	7	61	593399.949	0.005	67.2577	a	696.88
69	4	65	68	4	64	593709.797	-0.002	68.4769	a	697.50
67	6	61	66	6	60	593733.846	-0.017	66.5116	a	672.92
68	8	61	67	8	60	593819.022	0.002	67.0614	a	706.62
28	9	20	27	8	19	594076.268	-0.109	11.3955	b	153.82
68	5	63	67	5	62	594778.487	-0.047	67.4553	a	686.51
70	4	67	69	4	66	594790.387	0.030	69.5615	a	706.48
70	3	67	69	3	66	594846.478	0.029	69.5618	a	706.47
16	15	1	16	14	2	594988.033	0.004	1.9035	b	174.17
70	15	55	70	14	56	594998.899	0.036	36.2480	b	855.50
17	15	3	17	14	4	595022.247	0.059	2.7799	b	179.11
18	15	3	18	14	4	595057.803	0.012	3.6172	b	184.33
19	15	5	19	14	6	595094.759	0.019	4.4216	b	189.85
14	12	2	13	11	3	595107.938	-0.002	11.5765	b	109.67
14	12	3	13	11	2	595107.938	-0.002	11.5765	b	109.67
20	15	6	20	14	7	595132.984	0.050	5.1980	b	195.66
21	15	7	21	14	8	595172.303	0.037	5.9505	b	201.76
24	15	10	24	14	11	595295.986	0.029	8.0954	b	221.80
25	15	11	25	14	12	595338.674	-0.006	8.7807	b	229.07
67	15	53	67	14	54	595367.963	0.016	34.3976	b	795.55
26	15	12	26	14	13	595381.949	0.015	9.4541	b	236.62
27	15	13	27	14	14	595425.581	-0.004	10.1173	b	244.46
28	15	14	28	14	15	595469.514	0.025	10.7713	b	252.59
66	15	52	66	14	53	595472.421	0.073	33.7845	b	776.14
29	15	15	29	14	16	595513.499	-0.004	11.4173	b	261.01
30	15	16	30	14	17	595557.455	-0.020	12.0562	b	269.72
65	15	51	65	14	52	595568.011	0.029	33.1731	b	757.02
31	15	17	31	14	18	595601.268	0.018	12.6888	b	278.72
33	8	25	32	7	26	595621.682	-0.075	11.5080	b	187.11
32	15	18	32	14	19	595644.682	0.013	13.3159	b	288.02
64	15	50	64	14	51	595655.185	0.013	32.5634	b	738.19
33	15	19	33	14	20	595687.560	-0.007	13.9381	b	297.60
34	15	20	34	14	21	595729.769	-0.006	14.5560	b	307.47
63	15	49	63	14	50	595734.256	0.027	31.9553	b	719.64
35	15	21	35	14	22	595771.096	-0.023	15.1701	b	317.63
62	15	48	62	14	49	595805.463	-0.003	31.3486	b	701.38
36	15	22	36	14	23	595811.414	-0.008	15.7808	b	328.08
37	15	23	37	14	24	595850.494	-0.006	16.3886	b	338.82
61	15	47	61	14	48	595869.196	0.012	30.7435	b	683.41
39	15	25	39	14	26	595924.196	-0.035	17.5970	b	361.17
60	15	46	60	14	47	595925.732	0.049	30.1397	b	665.73
68	8	60	67	8	59	595934.997	0.041	67.0696	a	706.95
40	15	26	40	14	27	595958.486	-0.010	18.1981	b	372.78
59	15	45	59	14	46	595975.263	0.005	29.5372	b	648.34
41	15	27	41	14	28	595990.736	-0.026	18.7977	b	384.68

continued on next page

Table 6 Measured transitions of CH_2DCH_2CN out-of-plane- continued from previous page

Transition J'	K'a	K'c	J"	K"a	K"c	Obs. Freq. (MHz)	obs.- calc. (MHz)	S	Dipole	E_l (cm^{-1})
58	15	44	58	14	45	596018.201	0.004	28.9359	b	631.24
42	15	28	42	14	29	596020.842	0.018	19.3959	b	396.87
43	15	29	43	14	30	596048.457	-0.016	19.9930	b	409.35
57	15	43	57	14	44	596054.842	0.057	28.3358	b	614.42
44	15	30	44	14	31	596073.459	-0.036	20.5892	b	422.12
56	15	42	56	14	43	596085.311	0.009	27.7367	b	597.90
45	15	31	45	14	32	596095.657	-0.016	21.1848	b	435.18
55	15	41	55	14	42	596110.019	-0.002	27.1385	b	581.66
46	15	32	46	14	33	596114.773	-0.012	21.7798	b	448.52
54	15	40	54	14	41	596129.186	-0.029	26.5412	b	565.71
47	15	33	47	14	34	596130.619	0.015	22.3745	b	462.16
71	3	69	70	3	68	596623.510	0.027	70.6692	a	714.15
71	2	69	70	2	68	596626.020	0.034	70.6692	a	714.15
19	11	9	18	10	8	597900.664	-0.033	11.3193	b	118.47
19	11	8	18	10	9	597900.664	-0.033	11.3193	b	118.47
72	2	71	71	2	70	598553.381	0.000	71.7923	a	720.76
72	1	71	71	1	70	598553.381	-0.062	71.7923	a	720.76
69	6	64	68	6	63	598564.534	0.000	68.3857	a	707.40
69	17	53	68	17	52	598934.793	0.005	64.8151	a	878.96
69	16	54	68	16	53	598945.751	0.012	65.2936	a	856.34
69	18	52	68	18	51	598964.568	0.016	64.3077	a	902.93
69	15	55	68	15	54	599006.376	0.006	65.7431	a	835.10
69	19	51	68	19	50	599028.510	0.028	63.7712	a	928.26
69	20	50	68	20	49	599121.682	0.000	63.2059	a	954.94
69	14	56	68	14	55	599129.303	0.018	66.1636	a	815.25
69	21	49	68	21	48	599240.430	0.012	62.6115	a	982.95
69	13	57	68	13	56	599332.834	0.017	66.5553	a	796.79
69	13	56	68	13	55	599332.834	0.009	66.5553	a	796.79
69	22	48	68	22	47	599381.774	-0.019	61.9882	a	1012.29
69	23	47	68	23	46	599543.527	0.006	61.3359	a	1042.96
69	12	58	68	12	57	599644.852	0.106	66.9180	a	779.75
69	12	57	68	12	56	599644.852	-0.067	66.9180	a	779.75
69	24	46	68	24	45	599723.800	0.023	60.6546	a	1074.94
72	9	64	71	9	63	627937.473	0.017	70.8821	a	798.55
71	7	64	70	7	63	628465.846	-0.017	70.3880	a	759.72
72	8	65	71	8	64	628562.157	-0.008	71.1101	a	787.59
32	9	24	31	8	23	628618.468	-0.123	12.1168	b	188.10
72	9	63	71	9	62	628623.719	0.026	70.8840	a	798.65
75	3	73	74	3	72	629019.411	0.101	74.6680	a	795.38
76	1	75	75	1	74	630964.181	0.130	75.7922	a	802.25
73	6	68	72	6	67	631400.183	0.024	72.3839	a	788.91
72	8	64	71	8	63	632450.280	0.036	71.1328	a	788.28
77	1	77	76	1	76	632940.678	-0.025	76.9284	a	808.15
77	0	77	76	0	76	632940.678	-0.026	76.9284	a	808.15
73	17	57	72	17	56	633323.734	-0.010	69.0451	a	960.59
73	18	56	72	18	55	633336.726	-0.017	68.5655	a	984.57
73	16	58	72	16	57	633357.572	0.009	69.4975	a	937.98
73	19	55	72	19	54	633388.758	-0.015	68.0584	a	1009.91
73	15	59	72	15	58	633448.915	0.006	69.9224	a	916.75
73	20	54	72	20	53	633474.038	0.003	67.5239	a	1036.59
74	5	70	73	5	69	633495.614	0.106	73.4641	a	799.25
73	21	53	72	21	52	633588.123	0.003	66.9621	a	1064.62
73	14	60	72	14	59	633612.950	0.000	70.3201	a	896.91
73	22	52	72	22	51	633727.579	-0.037	66.3729	a	1093.98
74	4	70	73	4	69	633795.128	0.095	73.4661	a	799.19
73	13	61	72	13	60	633871.969	0.017	70.6904	a	878.48
73	13	60	72	13	59	633871.969	-0.016	70.6904	a	878.48
73	23	51	72	23	50	633889.780	-0.058	65.7563	a	1124.67
73	5	68	72	5	67	633914.899	-0.015	72.4113	a	788.32

continued on next page

Table 6 Measured transitions of CH_2DCH_2CN out-of-plane- continued from previous page

Transition						Obs. Freq.	obs.- calc.	S	Dipole	E_l
J'	K'$_a$	K'$_c$	J"	K"$_a$	K"$_c$	(MHz)	(MHz)			(cm^{-1})
73	24	50	72	24	49	634072.632	-0.012	65.1123	a	1156.68
73	26	48	72	26	47	634493.450	0.059	63.7422	a	1224.61
73	27	47	72	27	46	634728.724	-0.010	63.0160	a	1260.52
73	11	63	72	11	62	634830.430	0.004	71.3491	a	845.96
73	11	62	72	11	61	634838.965	-0.003	71.3492	a	845.96
73	29	44	72	29	43	635244.378	-0.006	61.4815	a	1336.19
18	16	3	18	15	4	635371.283	0.049	2.7935	b	204.18
19	16	4	19	15	5	635412.186	-0.007	3.6389	b	209.70
20	16	5	20	15	6	635454.716	-0.018	4.4522	b	215.51
21	16	6	21	15	7	635498.801	0.032	5.2379	b	221.62
22	16	7	22	15	8	635544.199	-0.007	6.0000	b	228.01
23	16	8	23	15	9	635590.985	0.034	6.7415	b	234.69
24	16	9	24	15	10	635638.921	0.018	7.4650	b	241.66
73	10	64	72	10	63	635650.542	0.007	71.6376	a	831.95
73	7	67	72	7	66	635706.496	-0.009	72.2835	a	798.68
26	16	11	26	15	12	635738.023	0.010	8.8671	b	256.48
73	10	63	72	10	62	635748.615	0.004	71.6379	a	831.96
27	16	12	27	15	13	635788.986	0.036	9.5491	b	264.32
14	13	1	13	12	2	635809.046	0.010	12.5178	b	125.46
14	13	2	13	12	1	635809.046	0.010	12.5178	b	125.46
28	16	13	28	15	14	635840.643	-0.014	10.2205	b	272.45
30	16	15	30	15	16	635945.873	-0.023	11.5358	b	289.59
31	16	16	31	15	17	635999.275	0.096	12.1817	b	298.59
32	16	17	32	15	18	636052.717	-0.012	12.8210	b	307.88
33	16	18	33	15	19	636106.396	-0.017	13.4543	b	317.47
34	16	19	34	15	20	636160.069	-0.024	14.0824	b	327.34
35	16	20	35	15	21	636213.617	-0.009	14.7058	b	337.50
36	16	21	36	15	22	636266.872	0.005	15.3249	b	347.96
37	16	22	37	15	23	636319.646	-0.020	15.9404	b	358.70
38	16	23	38	15	24	636371.892	0.022	16.5525	b	369.73
39	16	24	39	15	25	636423.292	-0.031	17.1617	b	381.05
40	16	24	40	15	25	636473.831	-0.034	17.7683	b	392.66
41	16	26	41	15	27	636523.316	-0.016	18.3727	b	404.56
42	16	27	42	15	28	636571.541	-0.016	18.9751	b	416.75
43	16	28	43	15	29	636618.360	-0.011	19.5757	b	429.23
44	16	29	44	15	30	636663.588	-0.011	20.1750	b	442.00
73	9	65	72	9	64	636669.624	-0.012	71.8977	a	819.50
69	16	54	69	15	55	636702.405	-0.002	35.1353	b	855.08
46	16	31	46	15	32	636748.571	-0.014	21.3699	b	468.41
67	16	52	67	15	53	636816.649	-0.005	33.9200	b	815.41
48	16	33	48	15	34	636825.044	-0.015	22.5614	b	495.97
49	16	34	49	15	35	636859.623	-0.010	23.1563	b	510.19
50	16	35	50	15	36	636891.488	-0.020	23.7509	b	524.69
51	16	36	51	15	37	636920.465	-0.022	24.3453	b	539.48
64	16	49	64	15	50	636937.983	-0.001	32.1071	b	758.05
52	16	36	52	15	37	636946.380	0.011	24.9396	b	554.57
63	16	48	63	15	49	636966.088	-0.003	31.5052	b	739.51
53	16	38	53	15	39	636968.944	-0.007	25.5340	b	569.94
55	16	40	55	15	41	637003.358	-0.024	26.7235	b	601.54
61	16	46	61	15	47	637005.301	0.033	30.3048	b	703.29
56	16	41	56	15	42	637014.784	-0.024	27.3188	b	617.78
60	16	44	60	15	45	637016.846	0.030	29.7060	b	685.61
57	16	42	57	15	43	637022.055	-0.031	27.9146	b	634.31
58	16	43	58	15	44	637024.991	-0.005	28.5110	b	651.12
73	8	66	72	8	65	637204.547	0.015	72.1208	a	808.56
72	7	65	71	7	64	637464.900	-0.021	71.4026	a	780.68
73	9	64	72	9	63	637502.418	0.016	71.9001	a	819.61
19	12	7	18	11	8	638734.557	-0.045	12.1303	b	132.90
19	12	8	18	11	7	638734.557	-0.045	12.1303	b	132.90

continued on next page

Table 6 Measured transitions of CH_2DCH_2CN out-of-plane- continued from previous page

		Transition				Obs. Freq.	obs.- calc.	S	Dipole	E_l
J'	K'$_a$	K'$_c$	J"	K"$_a$	K"$_c$	(MHz)	(MHz)			(cm^{-1})
78	1	78	77	1	77	641037.722	0.030	77.9284	a	829.26
78	0	78	77	0	77	641037.722	0.030	77.9284	a	829.26
24	11	14	23	10	13	641477.119	-0.106	12.1537	b	148.96
75	5	71	74	5	70	641578.592	0.114	74.4627	a	820.38
73	8	65	72	8	64	641645.995	-0.017	72.1495	a	809.38
74	5	69	73	5	68	641760.792	-0.005	73.4054	a	809.46
75	4	71	74	4	70	641827.842	0.112	74.4644	a	820.33
74	17	58	73	17	57	641912.245	-0.011	70.0988	a	981.71
74	18	57	73	18	56	641920.591	-0.029	69.6256	a	1005.69
74	16	59	73	16	58	641952.308	-0.027	70.5450	a	959.11
74	19	56	73	19	55	641969.272	-0.035	69.1253	a	1031.03
74	21	54	73	21	53	642164.880	-0.048	68.0439	a	1085.76
74	14	60	73	14	59	642227.254	-0.007	71.3566	a	918.05
74	14	61	73	14	60	642227.254	-0.005	71.3566	a	918.05
74	22	53	73	22	52	642303.680	-0.042	67.4626	a	1115.12
74	23	52	73	23	51	642465.814	-0.050	66.8543	a	1145.82
74	13	62	73	13	61	642501.346	0.010	71.7219	a	899.63
74	13	61	73	13	60	642501.346	-0.035	71.7219	a	899.63
39	4	36	39	3	37	182964.487	-0.034	19.1997	b	231.84
43	4	40	43	3	41	201516.181	-0.040	19.7405	b	279.35
70	2	68	69	3	67	588505.206	0.000	52.2606	b	694.52
70	3	68	69	2	67	588532.562	-0.018	52.2607	b	694.52
71	2	69	70	3	68	596613.897	0.024	53.2654	b	714.15
71	3	69	70	2	68	596635.621	0.025	53.2655	b	714.15

Table 7. Sample table of the predicted transitions of the ground vibrational state of $CH_3CH_2C^{15}N$

Transition J' (K'$_a$, K'$_c$) - J" (K"$_a$, K"$_c$)	Calc. Frequency (MHz)	Calc. Error (MHz)	S	Dipole	E_l (cm^{-1})
3 (1, 3) - 2 (1, 2)	25395.710	0.05	2.6666	A	1.62
4 (1, 3) - 4 (0, 4)	25554.136	0.05	4.3003	B	2.90
3 (0, 3) - 2 (0, 2)	26055.720	0.05	2.9994	A	0.87
3 (2, 2) - 2 (2, 1)	26083.623	0.05	1.6667	A	3.96
3 (2, 1) - 2 (2, 0)	26110.418	0.05	1.6667	A	3.96
3 (1, 2) - 2 (1, 1)	26761.502	0.05	2.6666	A	1.67
5 (1, 4) - 5 (0, 5)	26796.205	0.05	5.1207	B	4.34
6 (1, 5) - 6 (0, 6)	28339.734	0.05	5.8615	B	6.07
7 (1, 6) - 7 (0, 7)	30211.700	0.05	6.5105	B	8.09
6 (0, 6) - 5 (1, 5)	31961.207	0.05	2.8413	B	5.01
8 (1, 7) - 8 (0, 8)	32441.288	0.05	7.0582	B	10.39
4 (1, 4) - 3 (1, 3)	33853.023	0.05	3.7498	A	2.47
4 (0, 4) - 3 (0, 3)	34709.447	0.05	3.9986	A	1.74
4 (2, 3) - 3 (2, 2)	34772.635	0.05	2.9999	A	4.83
....					
59 (11, 48) - 58 (10, 49)	995315.711	0.06	18.4437	B	573.93
54 (9 , 45) - 54 (6, 48)	995592.250	0.07	0.1157	B	460.59
55 (6 , 50) - 54 (3, 51)	995665.199	0.07	1.2626	B	442.83
65 (10, 56) - 64 (9, 55)	996353.051	0.07	18.2257	B	666.68
65 (10, 55) - 64 (9, 56)	996527.533	0.07	18.2248	B	666.67
43 (14, 30) - 42 (13, 29)	996593.606	0.06	17.9466	B	392.48
43 (14, 29) - 42 (13, 30)	996593.606	0.06	17.9466	B	392.48
55 (5 , 51) - 54 (2, 52)	997274.064	0.14	1.0781	B	434.25
38 (15, 24) - 37 (14, 23)	998380.799	0.07	17.7294	B	355.17
38 (15, 23) - 37 (14, 24)	998380.799	0.07	17.7294	B	355.17
73 (9 , 65) - 72 (8, 64)	999104.052	0.08	17.3127	B	813.83
33 (16, 17) - 32 (15, 18)	999783.283	0.09	17.5672	B	326.61
33 (16, 18) - 32 (15, 17)	999783.283	0.09	17.5672	B	326.61
54 (12, 43) - 53 (11, 42)	999793.914	0.06	18.4736	B	508.77
54 (12, 42) - 53 (11, 43)	999793.924	0.06	18.4736	B	508.77

The entire table is available in electronic form on the CDS website http://cdsweb.u-strasbg.fr/cgi-bin/qcat?J/A+A/

Table 8. Sample table of the predicted transitions of the ground vibrational state of CH_3CHDCN

Transition J' (K'$_a$, K'$_c$) - J" (K"$_a$, K"$_c$)	Calc. Frequency (MHz)	Calc. Error (MHz)	S	Dipole	E_l (cm^{-1})
3 (1, 3) - 2 (1, 2)	25685.775	0.04	2.6666	A	1.53
6 (1, 5) - 6 (0, 6)	25869.041	0.04	5.6814	B	6.15
3 (0, 3) - 2 (0, 2)	26411.989	0.04	2.999	A	0.88
3 (2, 2) - 2 (2, 1)	26451.080	0.04	1.6667	A	3.56
3 (2, 1) - 2 (2, 0)	26489.353	0.04	1.6667	A	3.56
3 (1, 2) - 2 (1, 1)	27203.193	0.04	2.6666	A	1.58
7 (1, 6) - 7 (0, 7)	28031.338	0.04	6.2364	B	8.19
8 (1, 7) - 8 (0, 8)	30624.550	0.04	6.6694	B	10.52
9 (1, 8) - 9 (0, 9)	33684.164	0.04	6.9789	B	13.13
4 (1, 4) - 3 (1, 3)	34236.554	0.04	3.7497	A	2.38
4 (0, 4) - 3 (0, 3)	35171.176	0.04	3.9976	A	1.76
4 (2, 3) - 3 (2, 2)	35260.350	0.04	2.9999	A	4.44
19 (3 , 16) - 18 (4, 15)	35268.186	0.04	3.0105	B	61.09
4 (3, 2) - 3 (3, 1)	35287.953	0.04	1.7501	A	7.78
....					
69 (7 , 62) - 68 (6, 63)	995929.078	0.08	4.7701	B	716.57
72 (10, 62) - 71 (9, 63)	996138.578	0.08	17.3708	B	808.21
52 (14, 39) - 51 (13, 38)	996412.325	0.12	19.3529	B	503.06
52 (14, 38) - 51 (13, 39)	996412.325	0.12	19.3529	B	503.06
43 (16, 27) - 42 (15, 28)	996549.110	0.28	19.2560	B	415.75
43 (16, 28) - 42 (15, 27)	996549.110	0.28	19.2560	B	415.75
43 (6 , 37) - 42 (3, 40)	996760.122	0.06	0.10380	B	270.30
55 (7 , 49) - 54 (4, 50)	998269.602	0.05	1.14220	B	454.23
30 (19, 12) - 29 (18, 11)	998460.111	0.84	19.4241	B	343.54
30 (19, 11) - 29 (18, 12)	998460.111	0.84	19.4241	B	343.54
57 (13, 45) - 56 (12, 44)	999597.559	0.09	19.3721	B	565.96
57 (13, 44) - 56 (12, 45)	999597.576	0.09	19.3721	B	565.96
26 (26, 1) - 26 (25, 2)	999902.893	5.38	0.99380	B	516.84
26 (26, 0) - 26 (25, 1)	999902.893	5.38	0.99380	B	516.84
27 (26, 2) - 27 (25, 3)	999988.702	5.38	1.95270	B	524.81
27 (26, 1) - 27 (25, 2)	999988.702	5.38	1.95270	B	524.81

The entire table is available in electronic form on the CDS website http://cdsweb.u-strasbg.fr/cgi-bin/qcat?J/A+A/

Table 9. Sample table of the predicted transitions of the ground vibrational state of CH_2DCH_2CN in-plane

Transition J' (K'$_a$, K'$_c$) - J" (K"$_a$, K"$_c$)	Calc. Frequency (MHz)	Calc. Error (MHz)	S	Dipole	E_l (cm^{-1})
3 (0, 3) - 2 (0, 2)	25254.521	0.03	2.9995	A	0.84
3 (2, 2) - 2 (2, 1)	25278.632	0.03	1.6667	A	3.97
3 (2, 1) - 2 (2, 0)	25301.661	0.03	1.6667	A	3.97
4 (1, 3) - 4 (0, 4)	25630.983	0.03	4.3159	B	2.81
3 (1, 2) - 2 (1, 1)	25910.592	0.03	2.6666	A	1.65
5 (1, 4) - 5 (0, 5)	26781.045	0.03	5.1502	B	4.21
6 (1, 5) - 6 (0, 6)	28206.908	0.03	5.9108	B	5.89
7 (1, 6) - 7 (0, 7)	29932.070	0.03	6.5861	B	7.85
6 (0, 6) - 5 (1, 5)	29934.274	0.03	2.8151	B	4.89
8 (1, 7) - 8 (0, 8)	31982.230	0.03	7.1666	B	10.08
4 (1, 4) - 3 (1, 3)	32843.643	0.03	3.7498	A	2.43
4 (0, 4) - 3 (0, 3)	33645.594	0.03	3.9988	A	1.69
4 (2, 3) - 3 (2, 2)	33700.082	0.03	3	A	4.81
4 (3, 2) - 3 (3, 1)	33717.726	0.03	1.75	A	8.72
...					
52 (2 , 50) - 51 (1, 51)	996822.420	0.19	0.1924	B	358.79
81 (22, 59) - 81 (21, 60)	996989.852	0.59	39.3263	B	1276.12
81 (22, 60) - 81 (21, 61)	996989.852	0.59	39.3263	B	1276.12
77 (8 , 69) - 76 (7, 70)	997182.226	0.09	14.1792	B	863.19
82 (22, 61) - 82 (21, 62)	997192.282	0.6	39.908	B	1299.13
82 (22, 60) - 82 (21, 61)	997192.282	0.6	39.908	B	1299.13
83 (22, 61) - 83 (21, 62)	997394.781	0.62	40.4899	B	1322.41
83 (22, 62) - 83 (21, 63)	997394.781	0.62	40.4899	B	1322.41
84 (22, 62) - 84 (21, 63)	997597.271	0.63	41.072	B	1345.98
84 (22, 63) - 84 (21, 64)	997597.271	0.63	41.072	B	1345.98
58 (9 , 49) - 58 (6, 52)	997690.309	0.07	0.1427	B	511.44
75 (7 , 68) - 74 (6, 69)	998163.363	0.13	8.4514	B	810.36
33 (16, 17) - 32 (15, 18)	998409.251	0.04	17.5865	B	323.7
33 (16, 18) - 32 (15, 17)	998409.251	0.04	17.5865	B	323.7
52 (3 , 50) - 51 (0, 51)	999456.472	0.19	0.1921	B	358.79
55 (12, 44) - 54 (11, 43)	999572.240	0.03	18.7605	B	512.11
55 (12, 43) - 54 (11, 44)	999572.246	0.03	18.7605	B	512.11

The entire table is available in electronic form on the CDS website http://cdsweb.u-strasbg.fr/cgi-bin/qcat?J/A+A/

Table 10. Sample table of the predicted transitions of the ground vibrational state of CH_2DCH_2CN out-of-plane

Transition J' (K'$_a$, K'$_c$) - J" (K"$_a$, K"$_c$)	Calc. Frequency (MHz)	Calc. Error (MHz)	S	Dipole	E_l (cm^{-1})
3 (1, 3) - 2 (1, 2)	25366.325	0.03	2.6666	A	1.54
3 (0, 3) - 2 (0, 2)	26048.385	0.03	2.9992	A	0.87
3 (2, 2) - 2 (2, 1)	26081.805	0.03	1.6667	A	3.63
6 (1, 5) - 6 (0, 6)	26083.982	0.03	5.7568	B	6.07
3 (2, 1) - 2 (2, 0)	26114.266	0.03	1.6667	A	3.63
3 (1, 2) - 2 (1, 1)	26785.701	0.03	2.6666	A	1.58
7 (1, 6) - 7 (0, 7)	28074.467	0.03	6.3507	B	8.09
8 (1, 7) - 8 (0, 8)	30455.284	0.03	6.8307	B	10.38
9 (1, 8) - 9 (0, 9)	33259.094	0.03	7.193	B	12.96
4 (1, 4) - 3 (1, 3)	33812.231	0.03	3.7497	A	2.38
6 (0, 6) - 5 (1, 5)	34522.189	0.03	2.8968	B	4.92
4 (0, 4) - 3 (0, 3)	34693.075	0.03	3.998	A	1.74
4 (2, 3) - 3 (2, 2)	34769.082	0.03	2.9999	A	4.5
4 (3, 2) - 3 (3, 1)	34792.957	0.03	1.75	A	7.95
...					
72 (25, 47) - 72 (24, 48)	998737.270	0.4	33.1422	B	1156.68
73 (25, 49) - 73 (24, 50)	998938.927	0.41	33.7368	B	1177.83
73 (25, 48) - 73 (24, 49)	998938.927	0.41	33.7368	B	1177.83
66 (11, 56) - 65 (10, 55)	998943.870	0.03	18.9621	B	691.67
66 (11, 55) - 65 (10, 56)	999001.043	0.03	18.9619	B	691.67
74 (25, 49) - 74 (24, 50)	999141.512	0.42	34.3308	B	1199.26
74 (25, 50) - 74 (24, 51)	999141.512	0.42	34.3308	B	1199.26
75 (25, 50) - 75 (24, 51)	999344.959	0.43	34.9243	B	1220.99
75 (25, 51) - 75 (24, 52)	999344.959	0.43	34.9243	B	1220.99
53 (7, 47) - 52 (4, 48)	999517.559	0.04	0.6938	B	416.68
76 (25, 52) - 76 (24, 53)	999549.202	0.44	35.5172	B	1242.99
76 (25, 51) - 76 (24, 52)	999549.202	0.44	35.5172	B	1242.99
77 (25, 53) - 77 (24, 54)	999754.176	0.45	36.1097	B	1265.29
77 (25, 52) - 77 (24, 53)	999754.176	0.45	36.1097	B	1265.29
78 (25, 53) - 78 (24, 54)	999959.814	0.46	36.7019	B	1287.87
78 (25, 54) - 78 (24, 55)	999959.814	0.46	36.7019	B	1287.87

The entire table is available in electronic form on the CDS website http://cdsweb.u-strasbg.fr/cgi-bin/qcat?J/A+A/

Table 11. Observed transitions of $CH_3CH_2C^{15}N$ (without high blend) in the frequency range of the Orion KL survey. Column 1 indicates the transition, column 2 provides the assumed rest frequency, column 3 the line strength, column 4 the energy of the upper level, column 5 the observed (centroid) frequencies assuming that the radial velocities relative to LSR are 5 km s^{-1}, column 6 the observed peak line temperature of main beam, and column 7 indicates the main beam temperature derived from the model.

Transitions J_{K_a,K_c}	Pred. Freq. (MHz)	S_{ij}	E_u/k (K)	Obs. Freq. (MHz)	Obs. T_{mb} (K)	Model T_{mb} (K)
$10_{6,5}$-$9_{6,4}$	87007.366	6.40	63.0	87007.2	0.044	0.011
$10_{6,4}$-$9_{6,3}$	87007.366	6.40	63.0	[1]		
$10_{7,4}$-$9_{7,3}$	87010.616	5.10	77.4	87010.3	0.024	0.015
$10_{7,3}$-$9_{7,2}$	87010.616	5.10	77.4	[1]		
$10_{5,6}$-$9_{5,5}$	87011.913	7.50	50.8	[1]		
$10_{5,5}$-$9_{5,4}$	87011.919	7.50	50.8	[1]		
$10_{8,2}$-$9_{8,1}$	87018.779	3.60	94.1	87019.2	0.026	0.005
$10_{8,3}$-$9_{8,2}$	87018.779	3.60	94.1	[1]		
$10_{3,7}$-$9_{3,6}$	87114.933	9.10	33.0	87114.2	0.070[2]	0.009
$10_{2,8}$-$9_{2,7}$	87815.417	9.60	27.5	87814.4	0.015	0.010
$10_{1,9}$-$9_{1,8}$	88914.019	9.89	24.6	88914.3	0.015	0.011
$11_{1,11}$-$10_{1,10}$	92801.263	10.9	27.9	92803.2[2]	0.020	0.013
$11_{0,11}$-$10_{0,10}$	94252.099	11.0	27.3	94251.3	0.040[3]	0.014
$11_{2,10}$-$10_{2,9}$	95397.849	10.6	32.0	95398.2	0.010	0.013
$11_{4,7}$-$10_{4,6}$	95750.117	9.55	45.4	95750.2	0.009	0.015
$11_{3,8}$-$10_{3,7}$	95868.920	10.2	37.6	95868.2	0.015	0.012
$11_{2,9}$-$10_{2,8}$	96765.809	10.6	32.2	96764.2	0.024	0.014
$12_{0,12}$-$11_{0,11}$	102578.600	12.0	32.2	102577.1	0.042	0.018
$12_{4,9}$-$11_{4,8}$	104469.699	10.7	50.4	104470.1	0.059	0.017
$12_{4,8}$-$11_{4,7}$	104472.697	10.7	50.4	[1]		
$12_{3,10}$-$11_{3,9}$	104517.172	11.2	42.6	104517.2	0.027	0.017
$12_{2,10}$-$11_{2,9}$	105746.402	11.7	37.3	105748.1	0.036	0.019
$12_{1,11}$-$11_{1,10}$	106509.810	11.9	34.4	106511.1	0.041[2]	0.020
$13_{0,13}$-$12_{0,12}$	110865.655	13.0	37.6	110867.0	0.032[2]	0.024
$13_{2,12}$-$12_{2,11}$	112621.740	12.7	42.4	112621.0	0.027	0.024
$13_{6,8}$-$12_{6,7}$	113127.839	10.2	78.0	113128.0	0.130	0.034
$13_{6,7}$-$12_{6,6}$	113127.839	10.2	78.0	[1]		
$13_{8,6}$-$12_{8,5}$	113129.990	8.08	109.1	[1]		
$13_{8,5}$-$12_{8,4}$	113129.990	8.08	109.1	[1]		
$13_{4,9}$-$12_{4,8}$	113200.301	11.8	55.8	113201.0	0.107	0.021
$13_{3,11}$-$12_{3,10}$	113245.049	12.3	48.0	113243.9	0.095[2]	0.023
$15_{7,9}$-$14_{7,8}$	130537.903	11.7	104.6	130539.7	0.149[2]	0.054
$15_{7,8}$-$14_{7,7}$	130537.903	11.7	104.6	[1]		
$15_{8,8}$-$14_{8,7}$	130539.798	10.7	121.3	[1]		
$15_{8,7}$-$14_{8,6}$	130539.798	10.7	121.3	[1]		
$15_{6,10}$-$14_{6,9}$	130549.183	12.6	90.2	130549.8	0.052	0.070
$15_{6,9}$-$14_{6,8}$	130549.187	12.6	90.2	[1]		
$15_{9,6}$-$14_{9,5}$	130550.372	9.60	140.1	[1]		
$15_{9,7}$-$14_{9,4}$	130550.372	9.60	140.1	[1]		
$15_{10,6}$-$14_{10,5}$	130567.307	8.33	161.2	130567.7	0.049	0.022
$15_{10,5}$-$14_{10,4}$	130567.307	8.33	161.2	[1]		
$15_{12,3}$-$14_{12,2}$	130615.586	5.40	209.9	130614.7	0.042	0.010
$15_{12,4}$-$14_{12,3}$	130615.586	5.40	209.9	[1]		
$15_{4,11}$-$14_{4,10}$	130673.185	13.9	67.9	130672.7	0.073	0.034
$15_{1,14}$-$14_{1,13}$	132670.810	14.9	52.3	132670.7	0.130[4]	0.042
$15_{2,13}$-$14_{2,12}$	132800.381	14.7	55.1	132799.7	0.075	0.041
$16_{8,9}$-$15_{8,8}$	139245.508	12.0	127.9	139247.0	0.280[2]	0.098
$16_{8,8}$-$15_{8,7}$	139245.508	12.0	127.9	[1]		
$16_{7,10}$-$15_{7,9}$	139246.220	12.9	111.3	[1]		
$16_{7,9}$-$15_{7,8}$	139246.220	12.9	111.3	[1]		
$16_{6,11}$-$15_{6,10}$	139262.522	13.8	96.8	139263.3	0.086	0.067
$16_{6,10}$-$15_{6,9}$	139262.529	13.8	96.8	[1]		
$16_{10,7}$-$15_{10,6}$	139271.671	9.75	167.9	139270.8	0.078	0.029
$16_{10,6}$-$15_{10,5}$	139271.671	9.75	167.9	[1]		

continued on next page

Table 11 Observed transitions of $CH_3CH_2C^{15}N$– continued from previous page

Transitions J_{K_a,K_c}	Pred. Freq. (MHz)	S_{ij}	E_u/k (K)	Obs. Freq. (MHz)	Obs. T_{mb} (K)	Model T_{mb} (K)
$16_{5,12}$-$15_{5,11}$	139306.059	14.4	84.6	139305.8	0.293[2]	0.073
$16_{5,11}$-$15_{5,10}$	139306.594	14.4	84.6	[1]		
$16_{12,4}$-$15_{12,3}$	139321.451	7.00	216.6	139321.9	0.045	0.015
$16_{12,5}$-$15_{12,4}$	139321.451	7.00	216.6	[1]		
$16_{1,15}$-$15_{1,14}$	141313.454	15.9	59.1	141314.5	0.060	0.051
$17_{0,17}$-$16_{0,16}$	143750.890	16.9	62.8	143750.6	0.18[5]1	0.056
$17_{8,10}$-$16_{8,9}$	147951.800	13.2	135.0	147955.6	0.256	0.064
$17_{8,9}$-$16_{8,8}$	147951.800	13.2	135.0	[1]		
$17_{7,11}$-$16_{7,10}$	147955.646	14.1	118.4	[1]		0.074
$17_{7,10}$-$16_{7,9}$	147955.646	14.1	118.4	[1]		
$17_{9,9}$-$16_{9,8}$	147959.709	12.2	153.9	[1]		0.050
$17_{9,8}$-$16_{9,7}$	147959.709	12.2	153.9	[1]		
$17_{10,7}$-$16_{10,6}$	147976.004	11.1	175.0	147975.5	0.170	0.093
$17_{10,8}$-$16_{10,7}$	147976.004	11.1	175.0	[1]		
$17_{6,12}$-$16_{6,11}$	147977.798	14.9	103.9	147977.5	0.192[2]	
$17_{6,11}$-$16_{6,10}$	147977.813	14.9	103.9	[1]		
$17_{5,13}$-$16_{5,12}$	148032.124	15.5	91.7	148030.7	0.245	0.083
$17_{5,12}$-$16_{5,11}$	148033.058	15.5	91.7	[1]		
$17_{4,14}$-$16_{4,13}$	148139.616	16.1	81.7	148137.0	0.104[2]	0.053
$17_{3,15}$-$16_{3,14}$	148147.371	16.5	74.0	148146.9	0.155[2]	0.055
$17_{4,13}$-$16_{4,12}$	148174.997	16.1	81.7	148174.4	0.158[6]	0.051
$17_{3,14}$-$16_{3,13}$	148810.665	16.5	74.1	148810.5	0.080	0.055
$17_{1,16}$-$16_{1,15}$	149910.805	16.9	66.3	149909.5	0.177[2]	0.061
$17_{2,15}$-$16_{2,14}$	150846.477	16.8	69.1	150847.5	0.135	0.060
$18_{1,18}$-$17_{1,17}$	151161.544	17.9	70.3	151170.6	0.185[7]	0.064
$18_{9,10}$-$17_{9,9}$	156664.727	13.5	161.4	156663.4	0.298[2]	0.116
$18_{9,9}$-$17_{9,8}$	156664.727	13.5	161.4	[1]		
$18_{7,12}$-$17_{7,11}$	156666.249	15.3	125.9	[1]		
$18_{7,11}$-$17_{7,10}$	156666.250	15.3	125.9	[1]		
$18_{10,9}$-$17_{10,8}$	156680.304	12.4	182.5	156679.4	0.077	0.047
$18_{10,8}$-$17_{10,7}$	156680.304	12.4	182.5	[1]		
$18_{6,13}$-$17_{6,12}$	156695.130	16.0	111.5	156693.4	0.196[2]	0.097
$18_{6,12}$-$17_{6,11}$	156695.157	16.0	111.5	[1]		
$18_{4,14}$-$17_{4,13}$	156939.258	17.1	89.3	156938.4	0.133	0.060
$18_{3,15}$-$17_{3,14}$	157730.365	17.5	81.6	157729.4	0.060	0.065
$18_{2,16}$-$17_{2,15}$	159848.455	17.8	76.8	159847.4	0.105	0.071
$19_{2,18}$-$18_{2,17}$	163915.948	18.8	83.4	163916.3	0.160[8]	0.077
$19_{1,18}$-$18_{1,17}$	166956.959	18.9	81.9	166957.3	0.125	0.082
$20_{2,19}$-$19_{2,18}$	172402.881	19.8	91.7	172401.6	0.228	0.088
$20_{8,13}$-$19_{8,12}$	174074.508	16.8	158.8	174072.8	0.426[9]	0.166
$20_{8,12}$-$19_{8,11}$	174074.508	16.8	158.8	[1]		
$20_{9,12}$-$19_{9,11}$	174075.518	16.0	177.7	[1]		
$20_{9,11}$-$19_{9,10}$	174075.518	16.0	177.7	[1]		
$20_{7,14}$-$19_{7,13}$	174091.254	17.6	142.2	174090.3	0.345[10]	0.128
$20_{7,13}$-$19_{7,12}$	174091.255	17.6	142.2	[1]		
$23_{7,17}$-$22_{7,16}$	200239.252	20.9	169.8	200241.0	0.143	0.162
$23_{7,16}$-$22_{7,15}$	200239.261	20.9	169.8	[1]		
$23_{12,12}$-$22_{12,11}$	200251.101	16.7	275.1	200250.9	0.136	0.064
$23_{12,11}$-$22_{12,10}$	200251.101	16.7	275.1	[1]		
$23_{1,22}$-$22_{1,21}$	200425.284	22.9	117.9	200423.4[2]	0.152	0.125
$23_{16,7}$-$22_{16,6}$	200442.132	11.9	398.7	200441.0	0.016	0.020
$23_{16,8}$-$22_{16,7}$	200442.132	11.9	398.7	[1]		
$23_{4,20}$-$22_{4,19}$	200668.972	22.3	133.2	200670.9	0.173[10]	0.110
$23_{2,21}$-$22_{2,20}$	204419.525	22.8	121.6	204422.9[2]	0.132	0.128
$25_{0,25}$-$24_{0,24}$	209271.572	24.9	132.1	209272.1	0.367[10]	0.138
$24_{2,22}$-$23_{2,21}$	213217.376	23.8	131.8	213215.8	0.320[11]	0.139
$25_{2,24}$-$24_{2,23}$	214557.679	24.8	139.1	214558.3	0.165	0.140
$26_{1,26}$-$25_{1,25}$	217285.943	25.9	142.6	217285.7	0.253	0.147

continued on next page

Table 11 Observed transitions of $CH_3CH_2C^{15}N$– continued from previous page

Transitions J_{K_a,K_c}	Pred. Freq. (MHz)	S_{ij}	E_u/k (K)	Obs. Freq. (MHz)	Obs. T_{mb} (K)	Model T_{mb} (K)
$26_{0,26}$-$25_{0,25}$	217474.027	25.9	142.6	217473.3	0.207	0.147
$25_{9,17}$-$24_{9,16}$	217607.414	21.8	225.8	217609.5	0.323	0.228
$25_{9,16}$-$24_{9,15}$	217607.414	21.8	225.8	[1]		
$25_{10,16}$-$24_{10,15}$	217609.115	21.0	246.8	[1]		
$25_{10,15}$-$24_{10,14}$	217609.115	21.0	246.8	[1]		
$25_{11,15}$-$24_{11,14}$	217626.225	20.2	270.1	217626.9	0.320	0.255
$25_{11,14}$-$24_{11,13}$	217626.225	20.2	270.1	[1]		
$25_{8,18}$-$24_{8,17}$	217627.120	22.4	206.9	[1]		
$25_{8,17}$-$24_{8,16}$	217627.120	22.4	206.9	[1]		
$25_{7,19}$-$24_{7,18}$	217679.026	23.0	190.2	217679.4	0.217	0.191
$25_{7,18}$-$24_{7,17}$	217679.051	23.0	190.2	[1]		
$25_{5,21}$-$24_{5,20}$	217976.444	24.0	163.7	217975.7	0.086	0.119
$25_{3,22}$-$24_{3,21}$	221023.822	24.6	146.8	221024.4	0.162	0.142
$26_{1,25}$-$25_{1,24}$	225064.582	25.9	149.2	225063.1	0.218	0.152
$26_{6,21}$-$25_{6,20}$	226521.943	24.6	186.7	226524.4[12]	0.244	0.203
$26_{6,20}$-$25_{6,19}$	226523.621	24.6	186.7	[1]		
$26_{5,22}$-$25_{5,21}$	226737.488	25.0	174.5	226736.8	0.235[13]	0.127
$26_{4,22}$-$25_{4,21}$	227585.336	25.4	164.8	227585.5	0.498	0.139
$28_{1,28}$-$27_{1,27}$	233761.349	27.9	164.7	233762.4	0.239	0.163
$28_{0,28}$-$27_{0,27}$	233886.100	27.9	164.6	233885.3	0.151	0.164
$27_{3,25}$-$26_{3,24}$	234807.835	26.7	168.0	234807.4	0.325	0.154
$27_{10,18}$-$26_{10,17}$	235016.780	23.3	269.0	235015.4	0.150	0.146
$27_{10,17}$-$26_{10,16}$	235016.780	23.3	269.0	[1]		
$27_{4,24}$-$26_{4,23}$	235703.198	26.4	175.9	235703.2	0.156	0.146
$28_{3,26}$-$27_{3,25}$	243387.108	27.7	179.7	243385.6	0.207	0.161
$28_{10,19}$-$27_{10,18}$	243720.490	24.4	280.7	243720.2	0.217	0.152
$28_{10,18}$-$27_{10,17}$	243720.490	24.4	280.7	[1]		
$28_{9,20}$-$27_{9,19}$	243730.327	25.1	259.6	243730.2	0.362	0.289
$28_{9,19}$-$27_{9,18}$	243730.327	25.1	259.6	[1]		
$28_{11,18}$-$27_{11,17}$	243731.014	23.7	303.9	[1]		
$28_{11,17}$-$27_{11,16}$	243731.014	23.7	303.9	[1]		
$28_{12,17}$-$27_{12,16}$	243756.893	22.9	329.4	243756.3	0.200	0.102
$28_{12,16}$-$27_{12,15}$	243756.893	22.9	329.4	[1]		
$28_{6,23}$-$27_{6,22}$	244007.283	26.7	209.7	244007.2	0.427	0.149
$28_{6,22}$-$27_{6,21}$	244011.067	26.7	209.7	244010.2	0.432	0.148
$29_{6,24}$-$28_{6,23}$	252754.799	27.8	221.8	252755.2	0.456	0.139
$29_{6,23}$-$28_{6,22}$	252760.349	27.8	221.8	252760.1	0.402	0.137
$29_{5,25}$-$28_{5,24}$	253042.421	28.1	209.7	253041.7	0.252	0.147
$29_{4,25}$-$28_{4,24}$	254464.800	28.4	200.1	254464.2	0.291	0.160
$31_{1,31}$-$30_{1,30}$	258449.466	30.9	200.7	258449.2	0.204	0.180
$30_{6,24}$-$29_{6,23}$	261513.668	28.8	234.4	261512.9	0.278	0.140
$30_{2,28}$-$29_{2,27}$	264929.014	29.8	202.0	264929.9	0.156	0.182
$32_{0,32}$-$31_{0,31}$	266726.277	31.9	213.5	266725.0	0.369	0.183
$31_{3,29}$-$30_{3,28}$	269002.338	30.7	217.2	269002.9	0.660	0.175
$31_{8,24}$-$30_{8,23}$	269919.627	28.9	278.3	269918.9	0.191	0.224
$31_{8,23}$-$30_{8,22}$	269919.638	28.9	278.3	[1]		
$31_{5,27}$-$30_{5,26}$	270593.584	30.2	235.3	270592.9	0.262	0.155
$31_{4,28}$-$30_{4,27}$	270656.392	30.5	225.4	270655.9	0.390	0.167
$31_{5,26}$-$30_{5,25}$	270792.922	30.2	235.3	270791.9	0.357	0.155
$33_{0,33}$-$32_{0,32}$	274937.410	32.9	226.7	274936.8	0.277[14]	0.185
$32_{11,22}$-$31_{11,21}$	278531.537	28.2	354.9	278530.1	0.736	0.247
$32_{11,21}$-$31_{11,20}$	278531.537	28.2	354.9	[1]		
$32_{10,23}$-$31_{10,22}$	278534.350	28.9	331.6	[1]		
$32_{10,22}$-$31_{10,21}$	278534.350	28.9	331.6	[1]		
$32_{4,29}$-$31_{4,28}$	279370.232	31.5	238.8	279270.2	0.556	0.301
$32_{5,28}$-$31_{5,27}$	279371.886	31.2	248.7	[1]		
$32_{5,27}$-$31_{5,26}$	279633.253	31.2	248.7	279632.8	0.384	0.157

continued on next page

Table 11 Observed transitions of $CH_3CH_2C^{15}N$– continued from previous page

Transitions J_{K_a,K_c}	Pred. Freq. (MHz)	S_{ij}	E_u/k (K)	Obs. Freq. (MHz)	Obs. T_{mb} (K)	Model T_{mb} (K)

[1] blended with the last one
[2] blended with unidentified line
[3] blended with $^{34}SO_2$
[4] blended with CH_3OCOH
[5] blended with $^{13}CH_2CHCN$
[6] blended with CH_3OCH_3
[7] blended with $SO^{18}O$
[8] blended with c-C_2H_4O
[9] blended with $^{13}CH_3OH$ ν_t=1
[10] blended with CH_3COCH_3
[11] blended with $H^{15}NCO$
[12] blended with CH_3CH_2CN b type
[13] blended with CH_3OD
[14] blended with $H^{13}CCCN$ ν_7=2